A Constructive Introduction to Quantum Field Theory

Lecture 6: Φ^4_3 on the torus

I. The FBSDE in force coordinates, two renormalisations and the large-field problem

M. GUBINELLI
Mathematical Institute, University of Oxford

November 2026

Abstract

The last two lectures construct the massive Φ^4_3 measure on the three-dimensional torus with the forward–backward equations of Lecture 4. In this lecture we set up the problem. For the mass regulator the Polchinski process of Lecture 4 is a noisy observation of the terminal field, and its forecast is the posterior mean; this gives an exact FBSDE at every lattice cutoff. Its backward half is the force equation of Lecture 4 in the forecast coordinate. We cannot solve that equation, so we construct an explicit approximate force and write the exact FBSDE in the coordinates it defines: the *approximate forecast* Y and the *error* Z. The error is driven only by the failure of the approximate force to solve it. We explain why the approximate force needs two renormalisations, in two senses: a linearly and a logarithmically divergent mass counterterm, and two correction steps beyond one loop, which make the defect integrable in the backward equation. Finally we identify the large-field problem: the construction only controls fields of size $r_q = (q/\lambda)^{1/2}$, and must be extended to all fields without losing coercivity. The price is an error that is not small but lives on large fields. Lecture 7 controls it by a priori estimates on the FBSDE and removes the cutoffs.

The results presented in Lectures 4–7 were obtained recently, with the use of AI, in collaboration with Sarah-Jean Meyer.

Table of contents

Introduction . . . 2

10 The problem and the exact FBSDE . . . 3
10.1 Lattice, scales and notation . . . 3
The resolution parameter . . . 3
10.2 The cutoff measure and the goal . . . 4
10.3 The Polchinski process as a filter . . . 5
10.4 The exact force in the forecast coordinate . 6
10.5 Approximate forecast and error . . . 6
Reading (10.13) . . . 8
10.6 Why the Polchinski expansion is not enough . . . 8
The exact force is linear at large fields . . . 9
The field equation does not see the cube . 10
What clipping does to the Burgers equation . . . 10
Integrating the cube . . . 11
Exercises . . . 13

11 Renormalisation: why two of them . . . 14
What must be approximated . . . 14
Why we project . . . 14
11.1 Scales and power counting . . . 15
The basic loop estimate . . . 15
11.2 The seed: one loop . . . 16
11.3 Corrections and the mass . . . 17
Splitting the force equation . . . 17
The iteration as Picard steps . . . 18
Why the first spatial moment is the right quantity . . . 18
The resolvent receives the cancellation . . 19
From the free resolvent to the loop response . . . 19
Why the centred source is integrable 19
The vertex pays for the spatial moment . . 20
Integrating from infinity . . . 20
Computing the first correction . . . 20
Computing the second correction 21
Following a spatial distance through a loop . . . 21
Weighted comparisons and the scale integral . . . 22

The four-leg bound after two steps 22
The scalar mass 23
Why we stop at the second correction . . . 23
Closing the mass path 24
Two nonlinear steps, one scalar fixed point 24
Where the small factor comes from 25
Integrating and normalising the differences 25
Why the outer contraction loses no more derivatives 26
11.4 Two mass renormalisations 27
11.5 Two correction steps 28
11.6 The explicit counterterm 29
Exercises 30
12 The flow at large fields 30
12.1 The large-field problem 30
A scalar model 30
12.2 Clipping 31
12.3 The complete defect 31
Where the large-field error comes from . . 32
The coordinate correction 32
12.4 The force below the auxiliary scale 32
Exercises 33
References 33

Introduction

Lecture 4 formulated a programme ((7.7) and Figure 7.1): solve the FBSDE

$$\Phi_t = \int_0^t \dot{Q}_s F_s \, \mathrm{d}s + \int_0^t \dot{Q}_s^{1/2} \mathrm{d}W_s, \qquad F_t = \mathbb{E}_t[-D V_T(\Phi_T)],$$

with a renormalised interaction V_T, with estimates uniform in the ultraviolet cutoff, and take the limit. For Φ_3^4 the force F_t is not expected to converge to an integrable terminal value, and the naive estimates of the force diverge (Appendix A.2 of Lecture 5). In these two lectures we carry out a version of the programme on the unit torus $\mathbb{T}^3$. The guiding principle is the one of Section 8: do not estimate Φ and F directly, but pass to the forecast coordinate, in which the forward equation has no drift and the tree diagrams have been integrated exactly. Section 10.6 shows on one site what goes wrong with a frozen cube, and what integrating it gives: this motivates the form of the approximate force.

The plan. Figure 10.1 gives the plan: this lecture builds the approximate force $\bar{\mathcal{F}}$; Lecture 7 does the estimates and the limits. The emphasis is on the structure of the argument. We give complete proofs of the identities and of the scalar models of the estimates, and only describe the tensor estimates on the lattice. The point of view is that of [BCG26]; for other constructions of Φ_3^4 see [GJ73, FO76, BFS83, BG20, GH21].

What is proved. Theorem 10.2 holds for every coupling, every reference mass $q_0 > 0$ and every finite part r of the counterterm, on a fixed torus, with no smallness, and for an explicit counterterm whose finite part is arbitrary. Section 18.7 lists what is not proved. Detailed proofs of what these lectures cite or condense are in the Supplement.

The reference mass. The number $q_0 > 0$ is not an additional regulator: it is the squared mass $m^2 = q_0$ of the Gaussian reference $C = C_{q_0} = (q_0 - \Delta_N)^{-1}$. It must be positive even on the torus, where there is no infrared problem at large distances, because the constants are in the kernel of $-\Delta_N$, so that $(-\Delta_N)^{-1}$ does not exist. The counterterm cannot supply this positivity, since its finite part r is an arbitrary real number, negative values included. The measure ν_N depends on q_0 and μ_N only through $q_0 + \mu_N$, so the two parameters are redundant: one may fix q_0 once and for all, for instance $q_0 = 1$, and let r be the free mass parameter. The number q_0 is also where the scale starts: the Polchinski process runs over $q \in [q_0, \infty)$ and vanishes at $q = q_0$ (see (10.7)).

One auxiliary scale. The expansion of the force needs g_q small, and this happens above an auxiliary scale $q_* \geqslant 1$, depending on λ, q_0 and on the finite part. Below it the coefficients are frozen (Section 12.4), so the force, the system and the results hold at all scales, and no statement about ν depends on it.

Acknowledgements. The results presented in Lectures 4–7 are joint work with Sarah-Jean Meyer, obtained recently with the use of AI. M. Gubinelli is partly supported by UK Research and Innovation via the grant "StochFields" EP/Z534328/1 and by the Simons Collaboration on Probabilistic Paths to QFT. S.-J. Meyer is supported by the grant "StochFields" EP/Z534328/1.

10 The problem and the exact FBSDE

10.1 Lattice, scales and notation

Let N be an odd integer and $\Lambda_N = (N^{-1}\mathbb{Z}/\mathbb{Z})^3$ the periodic lattice of mesh N^{-1} in the unit torus. Let $H_N = \mathbb{R}^{\Lambda_N}$ with

$$\langle u, v\rangle = \int u\, v, \qquad \int f := N^{-3} \sum_{x\in\Lambda_N} f(x),$$

so that the volume is 1 and integrals approximate continuum integrals. The nearest-neighbour Laplacian is $\Delta_N u(x) = N^2 \sum_{i=1}^3 [u(x+e_i/N) + u(x-e_i/N) - 2u(x)]$; we usually drop the index N. A kernel $C(x,z)$ acts by

$$Cu(x) = \int C(x,z)\, u(z)\mathrm{d}z,$$

so the identity has kernel $N^3 1_{x=z}$, and

$$\mathrm{Tr}C = \int C(x,x)\mathrm{d}x, \qquad (\mathrm{diag}C)(x) = C(x,x), \qquad \|C\|_{\mathrm{row}} = \sup_x \int |C(x,z)|\mathrm{d}z.$$

The *row norm* $\|C\|_{\mathrm{row}}$ is the largest L^1 norm of a row of the kernel. It bounds the operator norm on L^∞, and for a symmetric kernel on every L^p, $1 \leqslant p \leqslant \infty$, by interpolation: $\|C\|_{p\to p} \leqslant \|C\|_{\mathrm{row}}$. M_f is multiplication by f, and $K + \lambda y^2$ means $K + \lambda M_{y^2}$. For a functional F on H_N, DF, D^2F, D^kF are its gradient and derivatives, as in Lecture 3. $\|u\|_p$ is the L^p norm for the measure $\int$.

The resolution parameter. Lecture 3 used a general covariance profile. Here we use the *mass-regulator profile* of Exercise 8.8 of Lecture 4: with $m^2 = q_0$ and $t \geqslant 0$,

$$\hat{Q}_t(k) = \frac{1}{|k|^2 + q_0} - \frac{1}{|k|^2 + q_0 + t^2}, \qquad \mathcal{R}_t = t^2.$$

It is convenient to parametrise the resolution by the squared regulator mass

$$q := q_0 + t^2 \in [q_0, \infty).$$

Set

$$K_q := q - \Delta_N, \qquad C_q := K_q^{-1}, \qquad C := C_{q_0} = (m^2 - \Delta_N)^{-1}. \tag{10.1}$$

In the notation of Lectures 3–4, with $T = \infty$ and using q instead of t as the resolution variable (so $\dot{Q}$ now means $\partial_q Q_q$),

$$Q_q = C - C_q, \qquad \partial_q Q_q = C_q^2, \qquad \dot{Q}^{1/2} = C_q, \qquad S_q = C_q, \qquad \mathcal{R}_q = q - q_0, \qquad \partial_q \mathcal{R}_q = 1. \tag{10.2}$$

So C_q is the covariance of the scales not yet resolved, and $K_q = S_q^{-1}$ is the precision of the posterior at resolution q under the free prior μ^C. The main properties of C_q are elementary.

Lemma 10.1. (Free resolvents) *For $q \geqslant q_0$ (constants depend on the lower bound only for scales below one), uniformly in N: C_q has a nonnegative kernel,*

$$C_q 1 = q^{-1} 1, \qquad \|C_q\|_{p\to p} = q^{-1} \text{ for } 1 \leqslant p \leqslant \infty, \tag{10.3}$$

and

$$a_2(q) := (C_q^2)(x,x) = \operatorname{Tr} C_q^2 \lesssim q^{-1/2} \wedge N^3 q^{-2}, \qquad \operatorname{Tr} C_q \lesssim N \wedge N^3 q^{-1}. \tag{10.4}$$

For $y \in H_N$ and $\lambda > 0$, the killed resolvent

$$G_q(y) = (K_q + \lambda y^2)^{-1}$$

satisfies

$$0 \leqslant G_q(y)(x,z) \leqslant C_q(x,z).$$

Proof. $C_q = \int_0^\infty \mathrm{e}^{-qs} \mathrm{e}^{s\Delta} \mathrm{d}s$ and $\mathrm{e}^{s\Delta}$ is the transition kernel of the lattice random walk. This gives positivity and the row sums. Killing the walk at rate λy^2 gives the comparison for G_q. The symbol of $-\Delta_N$ is comparable to $|k|^2$ on the centred frequency cube $n \in \{-\frac{N-1}{2}, \dots, \frac{N-1}{2}\}^3$ (symbol $4N^2 \sum_i \sin^2(\pi n_i/N)$, with $k = 2\pi n$), and

$$\sum_k (q + |k|^2)^{-2} \leqslant C \int_{\mathbb{R}^3} (q + |k|^2)^{-2} \mathrm{d}k = C q^{-1/2}.$$

Counting the N^3 modes gives the other bounds. □

The *bubble* $a_2(q)$ is the coincident-point variance of the shell at resolution q:

$$\partial_q \operatorname{Var}(X_q(x)) = a_2(q)$$

for the free field at resolution q, and

$$\int_{q_0}^\infty a_2 = \operatorname{Tr} C_{q_0} \asymp N$$

is the divergent variance of the lattice field.

10.2 The cutoff measure and the goal

Fix $\lambda > 0$. The interaction and the lattice measure are

$$U(\varphi) = \frac{\lambda}{12} \int \varphi^4, \qquad V_N(\varphi) = U(\varphi) + \frac{\mu_N}{2} \int \varphi^2, \qquad \nu_N(\mathrm{d}\varphi) = \frac{\mathrm{e}^{-V_N(\varphi)}}{Z_N} \mu^C(\mathrm{d}\varphi), \tag{10.5}$$

where μ^C is the centred Gaussian measure with covariance $C = C_{q_0}$ on H_N, and $\mu_N \in \mathbb{R}$ is a mass counterterm to be chosen. With this normalisation $D^2 U(y) = \lambda M_{y^2}$: the coupling is the curvature of the interaction, which is why we write $\lambda/12$. In Lecture 4 we wrote the interaction as

$$\frac{\lambda}{12} \int H_4(\varphi; c_T) + \gamma_T \int H_2(\varphi; c_T);$$

the coupling is the same, and the Wick ordering is now part of μ_N. For every real μ_N, ν_N is a probability measure with all moments, since the quartic term dominates.

Theorem 10.2. (Main result, informal) *Let $\lambda>0$, $q_0>0$, $r\in\mathbb{R}$, and*

$$\mu_N = r - \lambda \operatorname{Tr} C + \frac{2}{3}\lambda^2 \int C^3.$$

Then:

a) the laws ν_N, embedded in $H^{-s}(\mathbb{T}^3)$, $s>\frac{1}{2}$, converge along the whole sequence to a measure ν, and ν is an explicit density over the explicit flow from $Y_{q_0}=0$ (Theorem 18.5);

b) the forecast processes converge in law, along the whole sequence, tested at each scale and jointly with the terminal field, to a solution of a forward–backward system on $[q_0,\infty)$, $Y_{q_0}=0$, driven by a cylindrical Brownian motion, whose terminal value has the law ν; the forecast is $\psi_q = m_q(\Phi_q)$ with m_q continuous (Theorem 18.6);

c) ν has a renormalised variational formula (Theorem 18.12), and it satisfies the integration by parts formula of Theorem 18.8, in which the renormalised cube appears only tested in expectation, and it has quartic exponential tails for tested fields.

The bounds that prove (a) and (b) are uniform in N: this is *UV stability*. They are bounds on the *error* Z of an approximate forecast, defined below. We now set up the exact FBSDE at fixed N.

10.3 The Polchinski process as a filter

At fixed N everything in Sections 7–8 of Lecture 4 is a theorem. We need it in the profile (10.2), where the regulator is $q-q_0$ and the terminal resolution $q=\infty$.

Proposition 10.3. (The Polchinski process) *At every fixed N, the Polchinski process of Theorem 7.3 of Lecture 4 starts at $\Phi_{q_0}=0$ and solves*

$$\mathrm{d}\Phi_q = C_q^2 F_q \,\mathrm{d}q + C_q \,\mathrm{d}W_q, \qquad F_q = \mathbb{E}_q[-D V_N(\Phi_\infty)], \tag{10.6}$$

where W is a Brownian motion on H_N, $\mathbb{E}_q$ is the conditional expectation given $\mathcal{F}_q=\sigma(\Phi_s : s\leqslant q)$, and $\Phi_q\to\Phi_\infty\sim\nu_N$ as $q\to\infty$ (by (10.7) below; see the proof of Lemma 16.1).

Proposition 10.4. (Filtering) *At every fixed N, by Proposition 7.7 of Lecture 4:*

a) the Polchinski process is a noisy observation of the terminal field: there is a Brownian motion B on H_N, independent of Φ_∞, with

$$\Phi_q = (q-q_0) C_q \Phi_\infty + C_q B_{q-q_0}; \tag{10.7}$$

b) the forecast $\psi_q = \mathbb{E}_q\Phi_\infty = \Phi_q + C_q F_q$ is a smooth function of Φ_q, $\psi_q = m_q(\Phi_q)$, with $D m_q = \mathrm{Cov}_q K_q$ invertible, where $\mathrm{Cov}_q = \mathrm{Cov}(\Phi_\infty|\mathcal{F}_q) > 0$;

c) W is the innovation of the filter, and

$$\mathrm{d}\psi_q = \mathrm{Cov}_q \,\mathrm{d}W_q. \tag{10.8}$$

Proof. In this profile $J_q=(q-q_0)C_q$ and $S_q=C_q$, so (a) is the bridge (7.14) and (c) the filter equation of Lecture 4. For (b), the conditional law of Φ_∞ is ν_N tilted by $\exp(\langle K_q\Phi_q,\varphi\rangle - \frac{q-q_0}{2}\|\varphi\|_2^2)$ by (7.16): an exponential family in $K_q\Phi_q$, whose mean has derivative the covariance. □

The *noise* of the forecast is the conditional expectation of the bridge noise: taking $\mathbb{E}_q$ in (10.7),

$$\omega_q := K_q\Phi_q - (q-q_0)\psi_q = \mathbb{E}_q[B_{q-q_0}],$$

a function of the field, $\omega_q = \omega_q(\Phi_q)$ with $\omega_q(x) = K_q x - (q-q_0)m_q(x)$. It is the noise of the field equation of Lecture 5 in this profile, and it is sub-Gaussian whatever the interaction (Proposition 9.6 of Lecture 5, Lemma 13.2 of Lecture 7).

10.4 The exact force in the forecast coordinate

By Proposition 10.4(b) the map $\Phi_q \mapsto \psi_q$ is invertible, and we define the **exact force in the forecast coordinate** $\mathcal{F}_q$ (not to be confused with the filtration) by

$$\Phi_q = \psi_q + C_q\mathcal{F}_q(\psi_q), \quad \text{i.e.} \quad K_q\Phi_q = K_q\psi_q + \mathcal{F}_q(\psi_q). \tag{10.9}$$

So $F_q = -\mathcal{F}_q(\psi_q)$, the force of Theorem 8.2 of Lecture 4, and the second form is the field equation in the forecast coordinate. We write $\mathrm{Ctr}_E T$ for the contraction of two slots of a tensor T with a kernel E, and $H_q^{\mathrm{ex}}(y) = (K_q + D\mathcal{F}_q(y))^{-1}$.

Proposition 10.5. (The force equation with a mass regulator) *At fixed N, $\mathcal{F}_q$ is smooth, $D\mathcal{F}_q$ is symmetric, $K_q + D\mathcal{F}_q > 0$, and*

$$\partial_q\mathcal{F}_q(y) + \frac{1}{2}\mathrm{Ctr}_{H_q^{\mathrm{ex}}(y)^2}D^2\mathcal{F}_q(y) = 0, \quad \mathrm{Cov}_q = H_q^{\mathrm{ex}}(\psi_q). \tag{10.10}$$

Proof. Differentiating (10.9) in ψ and using $Dm_q = \mathrm{Cov}_q K_q$ gives $K_q + D\mathcal{F}_q(\psi_q) = \mathrm{Cov}_q^{-1}$. Apply Itô's formula to $\Phi_q = \psi_q + C_q\mathcal{F}_q(\psi_q)$ with (10.6), (10.8) and $\mathrm{d}C_q = -C_q^2\,\mathrm{d}q$: the martingale parts agree, and the drifts differ by C_q times the left side of (10.10). At fixed N the forecast has full support, so this holds for all y. □

This is the derivative of the Wetterich equation of Lecture 4 (Exercise 10.1). It is an identity about the unknown ν_N, not a construction. But since

$$\mathrm{d}\psi_q = H_q^{\mathrm{ex}}(\psi_q)\,\mathrm{d}W_q,$$

an approximate force gives approximate forecast coordinates, with an error governed by how badly it fails to solve (10.10).

10.5 Approximate forecast and error

Let $\bar{\mathcal{F}}_q$ be, for $q \geqslant q_0$, an odd map on H_N, continuous and piecewise smooth in q and y, with $D\bar{\mathcal{F}}_q$ symmetric and $K_q + D\bar{\mathcal{F}}_q \geqslant \bar{c}_q I$ with $\bar{c}_q > 0$. Define the approximate response, the **force defect** and its drift

$$H_q(y) := (K_q + D\bar{\mathcal{F}}_q(y))^{-1},$$

$$\mathcal{D}_q(y) := \partial_q\bar{\mathcal{F}}_q(y) + \frac{1}{2}\mathrm{Ctr}_{H_q(y)^2}D^2\bar{\mathcal{F}}_q(y), \quad b_q(y) := -H_q(y)\mathcal{D}_q(y). \tag{10.11}$$

The defect is the failure of $\bar{\mathcal{F}}$ to solve (10.10). The map $y \mapsto y + C_q\bar{\mathcal{F}}_q(y)$ is a bijection of H_N. Define the approximate forecast and the error by

$$Y_q + C_q\bar{\mathcal{F}}_q(Y_q) = \Phi_q, \quad Z_q := \psi_q - Y_q, \quad \Xi_q := \mathrm{Cov}_q - H_q(Y_q). \tag{10.12}$$

Equivalently Y_q solves the approximate coordinate equation

$$K_q\Phi_q = K_qY_q + \bar{\mathcal{F}}_q(Y_q),$$

which is (10.9) with $\bar{\mathcal{F}}$ in place of $\mathcal{F}$. If $\bar{\mathcal{F}}=\mathcal{F}$ then $Y=\psi$, $Z=0$, $\mathcal{D}=0$ and $b=0$.

Theorem 10.6. (The FBSDE in approximate forecast coordinates) *At every fixed N,*

$$\begin{aligned} \mathrm{d}Y_q &= [b_q(Y_q) + H_q(Y_q)\,Z_q]\mathrm{d}q + H_q(Y_q)\,\mathrm{d}W_q, \\ \mathrm{d}Z_q &= -[b_q(Y_q) + H_q(Y_q)\,Z_q]\mathrm{d}q + \Xi_q\,\mathrm{d}W_q, \end{aligned} \tag{10.13}$$

for $q \geqslant q_0$, and $Y+Z=\psi$ is the martingale $\int \mathrm{Cov}\,\mathrm{d}W$.

Proof. Y_q is a smooth function of (q,Φ_q), so it is an Itô process, $\mathrm{d}Y=\beta\,\mathrm{d}q + A\,\mathrm{d}W$. Apply Itô's formula to $Y_q + C_q\bar{\mathcal{F}}_q(Y_q)=\Phi_q$, with (10.6) and $\mathrm{d}C_q=-C_q^2\,\mathrm{d}q$, and multiply by K_q: the martingale parts give $(K+D\bar{\mathcal{F}})A=I$, so $A=H$, and the drifts give

$$(K+D\bar{\mathcal{F}})\beta = CF + C\bar{\mathcal{F}}(Y) - \partial_q\bar{\mathcal{F}} - \frac{1}{2}C\mathrm{tr}_{H^2}D^2\bar{\mathcal{F}} = \psi - Y - \mathcal{D},$$

since $CF=\psi-\Phi$ and $C\bar{\mathcal{F}}(Y)=\Phi-Y$. Hence $\beta = H(\psi - Y - \mathcal{D}) = HZ + b$, which is the first equation. The second is $\mathrm{d}Z=\mathrm{d}\psi-\mathrm{d}Y$ and (10.8). The computation uses no initial value. At the reference scale $\Phi_{q_0}=0$, so $Y_{q_0}=0$ by oddness. □

Remark. (Canonical coordinates between Polchinski and Wetterich) The construction is an exact change of coordinates for any admissible $\bar{\mathcal{F}}$, whether or not it approximates the exact force. Symmetry of its derivative gives a primitive $\bar{\mathcal{F}}_q = D\bar{\Gamma}_q$. Set

$$\mathcal{U}_q(y) = \frac{1}{2}\langle y, K_q y\rangle + \bar{\Gamma}_q(y), \qquad j_q = K_q\Phi_q.$$

Coercivity makes $\mathcal{U}_q$ strictly convex, and the coordinate equation is $j_q = D\mathcal{U}_q(Y_q)$, or $Y_q = D\mathcal{U}_q^*(j_q)$, where $\mathcal{U}_q^*$ is the Legendre transform. At fixed q, regard j,ψ as conjugate variables and put $P=H_q(Y)^{-1}Z$. Then

$$\langle \psi, \mathrm{d}j\rangle = \langle P, \mathrm{d}Y\rangle + \mathrm{d}(\mathcal{U}_q^*(j)).$$

Here the differentials are in phase space, with the scale held fixed. Thus $(j,\psi)\mapsto(Y,P)$ is canonical; its type-two generating function is

$$S_q(j,P) = \mathcal{U}_q^*(j) + \langle D\mathcal{U}_q^*(j), P\rangle, \qquad \psi = D_jS_q, \quad Y = D_PS_q.$$

The primitive of $\bar{\mathcal{F}}$, together with the Gaussian quadratic term, therefore determines the canonical change. The conjugate momentum is $P=H^{-1}Z$, rather than Z itself. For $\bar{\mathcal{F}}=0$ one has $Y=\Phi$, $H=C$ and $Z=CF$: the forward equation is the Polchinski equation. For $\bar{\mathcal{F}}=\mathcal{F}=D\Gamma$ one has $Y=\psi$ and $Z=P=0$: the prediction field is a martingale with the exact Wetterich response. Intermediate choices are equally valid; for example $\bar{\Gamma}=\theta\Gamma$, $0\leqslant\theta\leqslant1$, preserves coercivity since $K+\theta D^2\Gamma=(1-\theta)K+\theta(K+D^2\Gamma)>0$. Moreover,

$$\mathcal{D}_q = D\Big(\partial_q\bar{\Gamma}_q - \frac{1}{2}\mathrm{Tr}H_q\Big).$$

The defect measures the failure of the chosen potential to solve Wetterich's equation, up to a field-independent normalisation. The error also depends on terminal data: the zero choice has zero defect but generally nonzero Z, and need not satisfy the stronger terminal matching used below.

Reading (10.13). The equation for Y is forward and explicit, once Z is known: its coefficients b, H are deterministic functions built from $\bar{\mathcal{F}}$. The equation for Z is backward. Its terminal condition is not imposed but *proved*: if $\bar{\mathcal{F}}_q$ matches the bare force as $q \to \infty$, then $qZ_q \to 0$ at each fixed N (Lemma 16.1). Its only source is the drift b, i.e. the force defect, transported by the propagator $\exp \int H$. So:

UV stability means that the explicit force $\bar{\mathcal{F}}$ computes the forecast up to an error Z which is small uniformly in N.

For this we need: (i) a force defect $\mathcal{D}$ integrable against the backward propagator, which is a deterministic renormalisation problem (Section 11); (ii) global coercivity of $\bar{\mathcal{F}}$, so that $H_q(y)$ is a good noise coefficient for all fields (Section 12); (iii) a priori estimates for the coupled system (Lecture 7). Figure 10.1 summarises the logic of the two lectures.

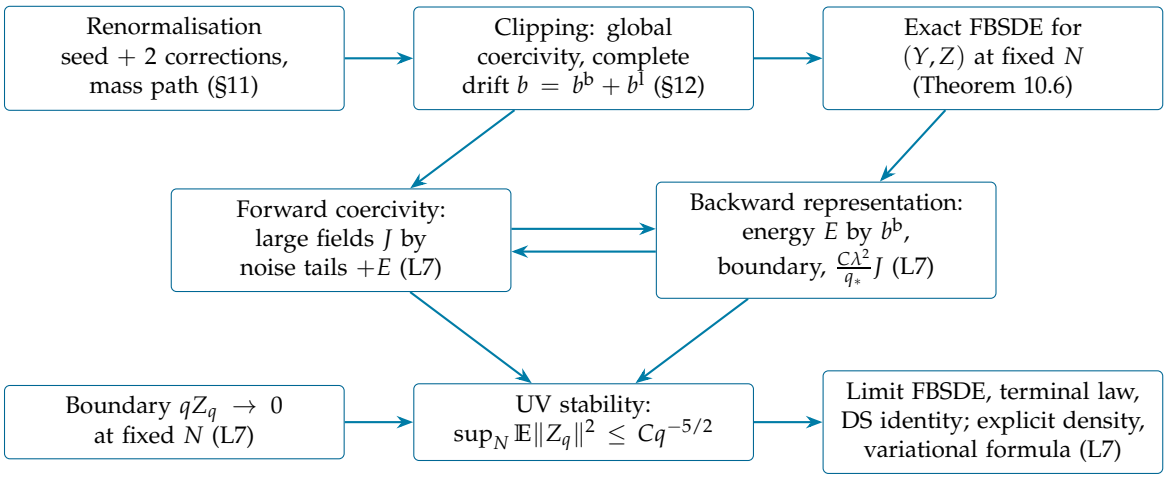


Figure 10.1. The structure of the construction (E, J: the energies of Lecture 7). The two arrows between the forward and backward estimates form the closed loop of Lecture 7: neither estimate closes on its own.

10.6 Why the Polchinski expansion is not enough

Before building the approximate force, we test on one site why it is written in the forecast coordinate. Lecture 4 gives two exact descriptions of the flow: the Burgers equation for the force F at the field Φ, and the force equation at the forecast ψ. We use the second, here and in Lecture 7. The first looks more economical, and the following programme is natural:

1. Keep the bare cube $-\frac{\lambda}{3}\varphi^3$ unclipped, so that the approximate force stays coercive at all fields.
2. Expand the rest of the force in perturbation theory and clip only these higher orders.
3. Pay for the clipping in the source of the equation for the remainder $R = F - f$, using the a priori estimates.

No change of coordinates would be needed.

Here we test the programme where everything can be computed: on one site. There is no spatial structure and no renormalisation, so whatever goes wrong has nothing to do with divergences.

Conventions. As in Exercise 10.4: $N = 1$, $\Delta = 0$, $K_q = q$, $V(\varphi) = \frac{\lambda}{12}\varphi^4$ and $r_q = (q/\lambda)^{1/2}$. We write $S = C_q = 1/q$ for the remaining covariance, and x for the value of the field at resolution q.

The exact force is linear at large fields. The exact force is the conditional mean of the bare force,

$$F_q(x) = -\frac{\lambda}{3}\mathbb{E}_x Y^3,$$

where $\mathbb{E}_x$ is the expectation for the probability density proportional to $e^{-\frac{\lambda}{12}y^4-\frac{q}{2}(y-x)^2}$. It solves the Burgers equation

$$\partial_q F + \frac{1}{2}S^2F'' + S^2FF' = 0. \tag{10.14}$$

Let $m_q(x) = \mathbb{E}_x Y$. Integrating by parts in y gives

$$F_q(x) = -\frac{\lambda}{3}\mathbb{E}_x Y^3 = q(m_q(x) - x). \tag{10.15}$$

This is Proposition 10.4(b): the posterior mean is the forecast, $\psi_q = m_q(\Phi_q)$. So F_q measures how far the forecast lies behind the field.

Lemma 10.7. (Posterior mean) *For all x and q,*

$$|m_q(x)| \leqslant 2(\lambda/3)^{-1/4} + 2(3q|x|/\lambda)^{1/3}.$$

Proof. Integrating the derivative of y times the density gives

$$\frac{\lambda}{3}\mathbb{E}_x Y^4 + q\mathbb{E}_x Y^2 - qx\mathbb{E}_x Y = 1.$$

With $M = (\mathbb{E}_x Y^4)^{1/4}$ this gives

$$\frac{\lambda}{3}M^4 \leqslant 1 + q|x|M,$$

and Young's inequality gives

$$\frac{\lambda}{6}M^4 \leqslant 1 + (q|x|)^{4/3}(2\lambda/3)^{-1/3}.$$

Finally $|m_q| \leqslant M$. □

Therefore, by (10.15), the two regimes of the force are

$$F_q(x) \to -\frac{\lambda}{3}x^3 \quad (\text{fixed } x, q \to \infty), \qquad F_q(x) = -qx + O(|x|^{1/3}) \quad (\text{fixed } q, |x| \to \infty). \tag{10.16}$$

The limits cannot be interchanged. The crossover is at $|x| \sim r_q$, where the cube equals the Gaussian restoring force: $\frac{\lambda}{3}r_q^3 \sim q\,r_q$. Beyond it the force is linear, because convolution with a Gaussian of variance S cannot produce a force steeper than x/S.

Proposition 10.8. (The remainder of a frozen cube) *Let*

$$f(x) = -\frac{\lambda}{3}x^3 + f_1(x)$$

with $f_1(x) = o(|x|^3)$, for instance linear terms plus bounded clipped corrections. At every fixed q, the remainder $R_q = F_q - f$ satisfies

$$\frac{3R_q(x)}{\lambda x^3} \to 1 \quad (|x| \to \infty).$$

So no estimate can make R a small fraction of the retained cube uniformly in the field. The cube in R is not a new counterterm, since there is nothing to renormalise here. It is the compensation for having frozen the leading term of a force that does not stay cubic.

The field equation does not see the cube. The field equation (18.20) of Lecture 7 on one site is

$$q_0\Phi_q = J_q F_q(\Phi_q) + \omega_q,$$

where $J_q = (q-q_0)/q$. Its noise is the conditional expectation of the bridge noise, so

$$\mathbb{E}\exp(h\omega_q) \leqslant \exp((q-q_0)h^2/2)$$

whatever the interaction (Lemma 13.2 of Lecture 7). With the frozen cube $f = -\frac{\lambda}{3}x^3$ the equation looks coercive:

$$q_0 x + J_q\frac{\lambda}{3}x^3 = J_q R_q(x) + \omega_q(x).$$

But by Proposition 10.8, $J_q R_q$ cancels the cube on the left side at large fields. Inserting (10.15) shows what is left:

$$q\,x = (q-q_0)m_q(x) + \omega_q(x). \tag{10.17}$$

There is still confinement, but it is linear, and it comes from the sublinear growth of m_q.

Proposition 10.9. (Tails on one site) *If $q^2 \geqslant 8\lambda$, then $|m_q(x)| \leqslant \frac{9}{10}|x|$ for $|x| \geqslant r_q$, and for $R \geqslant r_q$*

$$\mathbb{P}(|\Phi_q| \geqslant R) \leqslant 2\exp(-\frac{q^2R^2}{200(q-q_0)}).$$

Proof. The mean m has the sign of x, the density being an even density tilted by e^{qxy}; by symmetry take $x \geqslant r_q$, so that $\lambda x^2 \geqslant q$. Jensen's inequality in the identity of Lemma 10.7 gives

$$m\Big(\frac{\lambda}{3}m^3 + q(m-x)\Big) = \frac{\lambda}{3}m^4 + q\,m^2 - q\,x\,m \leqslant 1.$$

If $m > \frac{9}{10}x$, then, as $(9/10)^3/3 > 6/25$, the bracket exceeds $x(\frac{6}{25}\lambda x^2 - \frac{q}{10}) \geqslant \frac{7}{50}q\,x$, so the left side exceeds $\frac{9}{10}\cdot\frac{7}{50}q\,x^2 > \frac{qx^2}{8} \geqslant \frac{q^2}{8\lambda} \geqslant 1$, a contradiction. Hence, by (10.17), $|\omega_q(x)| \geqslant q|x| - (q-q_0)\frac{9}{10}|x| \geqslant \frac{q}{10}|x|$. On $\{|\Phi_q| \geqslant R\}$ we therefore have $|\omega_q| \geqslant q\,R/10$, and the sub-Gaussian bound $\mathbb{P}(|\omega_q| \geqslant a) \leqslant 2\mathrm{e}^{-a^2/(2(q-q_0))}$ with $a = q\,R/10$ concludes. □

At $R = r_q$ the exponent is at least $q^2/(200\lambda)$. This estimate treats the combined restoring force through the posterior moment. It never uses the cube as a coercive term against a remainder regarded as a source.

Remark 10.10. (This does not transfer to the lattice) With a linear term $a\,y$ in the force, Lemma 10.7 acquires the term $(3(q+a)_-/\lambda)^{1/2}$. On the lattice the bare mass makes a divergent and negative, so this elementary moment bound is not uniform until the renormalised cancellations have been built in. The scalar tail bound is therefore not an independent input for the field theory.

What clipping does to the Burgers equation. For a force f put $D_q = \partial_q + \frac{1}{2}S^2\partial_x^2$ and let $E_q(f) = D_q f + S^2 f f'$ be its Burgers defect, so $E_q(F_q) = 0$. Perturbation theory solves

$$D_q f_1 = 0, \quad D_q f_2 = -S^2 f_1 f_1',$$

with $f_1 = -\frac{\lambda}{3}(x^3 + 3S\,x)$, the cube and its Wick correction, and $f_2 = \frac{\lambda^2}{3}S\,x^5 + \dots$, the first tree. Keep f_1 unclipped and clip the correction: $f^c = f_1 + Cf_2$ with $Cf_2 = \kappa_q' \cdot f_2 \circ \kappa_q$, the clip κ_q of (12.1) below, a smooth odd map equal to the identity for $|x| \leqslant r_q$ and constant for $|x| \geqslant 2r_q$. Then

$$E_q(f^c) = (1-C)S^2 f_1 f_1' + [D_q, C]f_2 + S^2(f_1 Cf_2)' + S^2 Cf_2(Cf_2)'. \tag{10.18}$$

Without the clip only the last two terms, of higher order, would be present. The clip reintroduces a defect at exactly the order that f_2 was built to cancel. For $|x| \geqslant 2r_q$ we have $\mathcal{C} f_2 = 0$, so $f^c = f_1$, and the Burgers defect is exactly

$$E_q(x) = S^2 f_1(x) f_1'(x) = \frac{\lambda^2}{3} S^2 x^5 (1 + O(S/x^2)). \tag{10.19}$$

This is the price of the clipping. At the edge of the clip it is of order $(q/\lambda)^{1/2}$, which is not integrable in q, so it can only be paid through the small probability of reaching the clip. Along the exact process $\mathrm{d}\Phi_q = S^2 F_q(\Phi_q)\,\mathrm{d}q + S\,\mathrm{d}W_q$, Itô's formula gives for $R_q = F_q(\Phi_q) - f_q^c(\Phi_q)$ the equation

$$\mathrm{d}R_q = -[E_q(\Phi_q) + S^2 (f_q^c)'(\Phi_q) R_q]\,\mathrm{d}q + \Xi_q^R\,\mathrm{d}W_q. \tag{10.20}$$

The transport term has a favourable sign at large fields: $(f^c)' = -\lambda(x^2 + S)$ for $|x| \geqslant 2r_q$, which is the dissipation one hopes to use (near the clip the sign fails: on the ball the quintic takes over beyond $|x| \approx 0.77 r_q$). But at large fields the bracket is $\frac{\lambda^2}{3} S^2 x^5 - \lambda S^2 x^2 R$, and for the true $R \sim \frac{\lambda}{3} x^3$ the two terms cancel at leading order. The source and the dissipation are the same quantity, so estimating them separately gives nothing. To close, one would need, for instance, a signed estimate that retains this cancellation, or a tail bound for Φ obtained independently of R. On one site Proposition 10.9 is such a bound: the probability of reaching the clip is at most of order $\exp(-c\,q^2/\lambda)$, so in expectation the source is exponentially small, and the frozen cube is not ruled out there. But that bound comes from the posterior moment, and by the remark above it does not transfer. The field equation alone cannot replace it, since its restoring force is the cube and R together, which is what we are trying to estimate.

Going further in perturbation theory does not help: any finite depth of expansion leaves the same structure (Exercise 10.6), and we shall see in a moment that the series of trees stops converging inside r_q.

Integrating the cube. The term responsible for all this is the nonlinear transport in (10.14). So solve it exactly: let f_q solve the Burgers equation without diffusion,

$$\partial_q f + S^2 f f' = 0, \qquad f_\infty(x) = -\frac{\lambda}{3} x^3. \tag{10.21}$$

The characteristics give the solution in closed form.

Proposition 10.11. (The integrated cube) *For $x \in \mathbb{R}$, let $y = y_q(x)$ be the unique real root of $q\,y + \frac{\lambda}{3} y^3 = q\,x$. Then the solution of (10.21) is*

$$f_q(x) = -\frac{\lambda}{3} y_q(x)^3 = q(y_q(x) - x), \tag{10.22}$$

and it has the following properties.

- *a) **Variational form.** $y_q(x)$ is the minimiser of $\frac{\lambda}{12} y^4 + \frac{q}{2}(y - x)^2$, and $f_q = -\bar{V}_q'$ for the minimum value $\bar{V}_q(x)$.*
- *b) **Small fields.** $f_q(x) = q \sum_{k \geqslant 1} (-\frac{\lambda}{3q})^k c_k x^{2k+1}$ with $c_k = \frac{1}{2k+1} \frac{(3k)!}{k!(2k)!}$, so $f_q = -\frac{\lambda}{3} x^3 + \frac{\lambda^2}{3} S\, x^5 - \frac{4\lambda^3}{9} S^2 x^7 + \ldots$. This is the sum of the tree expansion. Its radius of convergence is $|x| = \frac{2}{3} r_q$.*
- *c) **Large fields.** $\frac{\lambda}{3}|y|^3 \leqslant q|x|$, so $f_q(x) = -q\,x + O(|x|^{1/3})$ at fixed q, as for the exact force, and $f_q' = -\lambda y^2/(1 + \lambda y^2/q) \leqslant 0$ for all x.*
- *d) **Defect.** f_q fails to solve Burgers by the diffusion term alone, which is q times the drift of Exercise 10.4:*

$$E_q = \frac{1}{2} S^2 f_q''(x) = q\, b_q(y_q(x)), \qquad b_q(y) = -\lambda y (q + \lambda y^2)^{-3}. \tag{10.23}$$

Proof. Differentiate $x = y + \frac{\lambda}{3} S y^3$ with $d = 1 + \lambda y^2/q$: $y' = 1/d$, $\partial_S y = -\frac{\lambda}{3} y^3/d$, $f' = -\lambda y^2/d$ and $f'' = -2\lambda y/d^3$. Hence $\partial_S f = \frac{\lambda^2}{3} y^5/d = f f'$, which is (10.21) as $\partial_q = -S^2 \partial_S$. For (a), the stationarity condition is $\frac{\lambda}{3} y^3 + q(y - x) = 0$. For (b), use Lagrange inversion on $y = x - \frac{\lambda}{3} S y^3$; the nearest singularity is where $d = 0$, that is at $y = \pm i r_q$, $x = \pm \frac{2}{3} i r_q$. Finally (c) and (d) are read off from the formulas, since $d = 1/(q H_q(y))$ with $H_q(y) = (q + \lambda y^2)^{-1}$. □

Item (b) explains why the depth of the expansion is not the issue. The tree series has the same complex singularity $y = \pm i r_q$ as the one-loop seed (Section 12.1 below), and its truncations at even k point outward at large fields.

The defect is now bounded for all fields, and it gives a global estimate.

Theorem 10.12. (Global error of the integrated cube) *Let* $C_* = 3 \sup_z |z|(1 + 3z^2)^{-3}$, *so* $C_* < \frac{1}{2}$. *For all* $q > 0$,

$$\sup_{x \in \mathbb{R}} |F_q(x) - f_q(x)| \leqslant 2 C_* \left(\frac{\lambda}{3q}\right)^{1/2}. \tag{10.24}$$

Proof. Use $S = 1/q$ as time, starting from $S = 0$. Subtracting, $\hat{R} = F - f$ solves the linear problem

$$\mathfrak{L} \hat{R} = \frac{1}{2} f'', \quad \mathfrak{L} = \partial_S - \frac{1}{2} \partial_x^2 - F \partial_x - f', \quad \hat{R}_0 = 0.$$

The zeroth-order coefficient has the good sign, as $-f' \geqslant 0$. With $z = (\lambda S/3)^{1/2} y$, the source obeys $\frac{1}{2}|f''| \leqslant C_* (\frac{\lambda}{3S})^{1/2}$, which is integrable at $S = 0$, so $\vartheta(S) = 2C_* (\lambda S/3)^{1/2}$ satisfies $\mathfrak{L}\vartheta \geqslant \frac{1}{2}|f''|$. To apply the maximum principle on the line, take $\chi = e^{3S}(1 + x^4)$. Then $\mathfrak{L}\chi \geqslant 0$, since $6x^2 \leqslant 3(1 + x^4)$ and $x F(x) \leqslant 0$; the last holds because $F = -\frac{\lambda}{3} \mathbb{E}_x Y^3$, and $\mathbb{E}_x Y^3$ has the sign of x, the density being an even density tilted by e^{qxy}. Both F and f grow at most cubically, uniformly for bounded S: $|f| \leqslant \frac{\lambda}{3}|x|^3$ since $|y| \leqslant |x|$, and $\frac{\lambda}{3} \mathbb{E}_x Y^6 + q \mathbb{E}_x Y^4 - q x \mathbb{E}_x Y^3 = 3 \mathbb{E}_x Y^2$ gives $\mathbb{E}_x Y^4 \leqslant (|x| + (3S)^{1/2})^4$, up to constants, hence $|F| \leqslant C\lambda(|x|^3 + S^{3/2})$. Also $\hat{R}$ is continuous at $S = 0$, since the posterior concentrates at x. So $\pm\hat{R} - \vartheta - \varepsilon\chi$ is negative on the boundary of a large cylinder, hence inside it. Let the cylinder grow and then $\varepsilon \to 0$. □

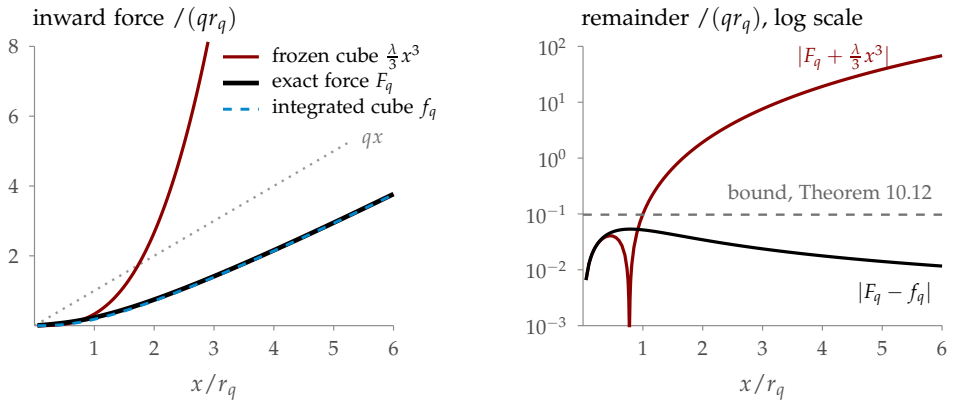


Figure 10.2. The force on one site, for $\lambda = 3$, $q = 4$. Left: the frozen cube leaves the exact force at $x \sim r_q$, while the integrated cube follows it at all fields: the two curves coincide at this scale, their difference being at most 0.06 in these units. Right, on a logarithmic scale: the remainder of the frozen cube grows like the cube itself, while the remainder of the integrated cube stays below the bound of Theorem 10.12. The dip of the frozen-cube curve at $x \approx 0.78 r_q$ is a sign change: the remainder is negative at small fields, where the Wick term $-\lambda S x$ dominates, and positive at large fields, where it approaches $\frac{\lambda}{3}x^3$.

The integrated cube is the forecast coordinate. The equation $q\,y+\frac{\lambda}{3}y^3=q\,x$, at $x=\Phi_q$, is the coordinate equation of Exercise 10.4, so $y_q(\Phi_q)=Y_q$. Equations (10.15) and (10.22) then say that $F_q-f_q=q(m_q-y_q)$: the remainder is K_qZ_q, and the error Z of (10.12) is the posterior mean minus the posterior mode. By (10.24), on one site $|Z_q|\leqslant 2C_*(\lambda/3)^{1/2}q^{-3/2}$ surely, for all fields.

Why the forecast coordinate has no such problem. In the variable y the bare cube does not flow at all: all the trees of (b) are contained in the map $x\mapsto y$. The second term of (10.10) is a loop, and the defect $\mathcal{D}_q(y)=\lambda y\,H_q(y)^2$ of $\bar{\mathcal{F}}_q=\frac{\lambda}{3}y^3$ is bounded by $\lambda^{1/2}q^{-3/2}$ for all y. This is why Section 12.2 below can leave the cube untouched and clip only the corrections: what is clipped consists of loops, not of trees whose large-field sum is forced to change the growth of the force. This removes the frozen-cube problem specifically: the clipping error of Section 12.3 below is still there, and it is what Lecture 7 pays for.

In the coordinate y the cube is genuine: $q\,y+\frac{\lambda}{3}y^3=q\,\Phi_q=(q-q_0)\psi_q+\omega_q$, i.e. $q_0y+\frac{\lambda}{3}y^3=\omega_q+(q-q_0)(\psi_q-y)$. This is the forecast equation of Lecture 5 with the explicit force in place of the exact one, the equation (13.3) of Lecture 7 on one site.

What the model points to. The scalar model points to the integration of the cube. The force equation in the forecast coordinate and the FBSDE of Theorem 10.6 are one way to organise it; another would keep the original field, with the force f_q given by the variational formula of (a), and work with the defect $\frac{1}{2}\mathrm{Ctr}_{C_q^2}D^2f_q$. On the lattice the variational formula still defines this force, with a nonlocal response, but its defect contains the loop contractions, starting with the tadpole, and must be renormalised. A complete proof along that route is not given in these lectures.

The scalar model proves less than a no-go theorem. It shows that a global estimate treating the remainder of a frozen cube as a small cubic perturbation is false. It does not show that every construction based on the Polchinski equation fails, nor does it give the asymptotics of the force on the lattice. There is also a limit to the integrated cube itself. With a linear term in the force, the map $y\mapsto y+S(\frac{\lambda}{3}y^3+ry)$ has derivative $1+S(r+\lambda y^2)$, which vanishes somewhere when $1+Sr<0$ (Exercise 10.7). A divergent negative mass cannot simply be placed inside this monotone map, and this is one reason why the mass correction M_q of (12.1) below is kept apart from the cube and is required to be small relative to K_q (Lemma 12.1 below).

Exercises

Exercise 10.1. (**Same force**) Show that $\bar{\mathcal{F}}_q$ of (10.9) coincides with the $\bar{\mathcal{F}}_t$ of (8.5) of Lecture 4 for the profile (10.2). Show that $\bar{\mathcal{F}}_q=D\Gamma_q$, where $\partial_q\Gamma_q=\frac{1}{2}\mathrm{Tr}\,H_q^{\mathrm{ex}}$, and that this agrees with the Wetterich equation (8.13), the difference being $-\frac{1}{2}\mathrm{Tr}\,C_q$.

Exercise 10.2. (**Gaussian case**) Let $V_N(\varphi)=\frac{a}{2}\|\varphi\|^2$, $a>0$. Compute ψ_q, Cov_q and $\bar{\mathcal{F}}_q$ explicitly, and check Proposition 10.4 and (10.10). Compare with Exercise 7.1.

Exercise 10.3. (**Bayes for the whole path**) Show that the conditional law of Φ_∞ given the whole path $(\Phi_s)_{s\leqslant q}$ depends only on Φ_q: the Polchinski process is a sufficient statistic for itself (Proposition 7.7(a) of Lecture 4).

Exercise 10.4. (**One site**) Take $N=1$ (one site, $\Delta=0$, $K_q=q$) and $\bar{\mathcal{F}}_q(y)=\frac{\lambda}{3}y^3$. (a) Show that Y_q is the real root of $q\,Y+\frac{\lambda}{3}Y^3=q\,\Phi_q$, and that $H_q(y)=(q+\lambda y^2)^{-1}$. Explain how large fields suppress the noise of Y. (b) Compute the defect $\mathcal{D}_q(y)=\lambda y(q+\lambda y^2)^{-2}$ and the drift $b_q(y)=-\lambda y(q+\lambda y^2)^{-3}$. Show that $|b_q(y)|\leqslant\lambda q^{-3}|y|$, and compare with Proposition 12.2: on one site $a_2(q)=q^{-2}$ instead of $q^{-1/2}$, and no renormalisation is needed.

Exercise 10.5. (**The defect**) Check (10.23) and integrate it: show that $\int_q^\infty q'\sup|b_{q'}|\,\mathrm{d}q'$ equals the right side of (10.24). Why does the integration of the cube turn the x^5 of (10.19) into a bounded function?

Exercise 10.6. (**Depth of the expansion**) Let f be any approximate force, $f^c = f + \delta$. Show that $E_q(f^c) = E_q(f) + D_q\delta + S^2(f\delta)' + S^2\delta\delta'$. Which terms are controlled by the smallness of the truncation defect $E_q(f)$? Take f the tree expansion up to order k, and δ the clipping of its terms beyond the cube. What replaces $\frac{\lambda^2}{3}S^2x^5$ in (10.19)?

Exercise 10.7. (**Negative mass**) For $r<0$, let $y \mapsto y + S(\frac{\lambda}{3}y^3 + ry)$. Show that it is monotone if and only if $1 + Sr \geqslant 0$. What happens to the minimiser in the variational formula when $1 + Sr < 0$, and to the solution of (10.21) with $f_\infty = -\frac{\lambda}{3}x^3 - rx$? Why does this not contradict the existence of the exact, smooth force F_q?

11 Renormalisation: why two of them

We now construct the force $\bar{\mathcal{F}}_q$ on bounded fields. The aim is an explicit approximation whose defect in the Wetterich force equation is small enough to drive the backward equation for Z. We do not need to solve the full nonlinear flow. We shall start from the bare cubic force, compute a one-loop seed, and improve it twice by inserting the preceding approximation into the equation. This section is deterministic: it uses no information on ν_N.

What must be approximated. The equation to approximate is

$$\partial_q \bar{\mathcal{F}}_q = -\frac{1}{2}\mathrm{Ctr}_{H_q^2} D^2 \bar{\mathcal{F}}_q, \qquad H_q = (K_q + D\bar{\mathcal{F}}_q)^{-1}.$$

At infinite resolution its boundary value is the bare force $U' + \mu_N y$, with $U'(y) = \frac{\lambda}{3}y^3$. A first idea is to insert U' on the right and integrate backwards from infinity. This does produce a useful nonlinear correction, but it also produces a linear term whose integral is not bounded uniformly in the lattice cutoff. For example, with $G_q(y) = (K_q + \lambda y^2)^{-1}$, the bare right-hand side at the site x is

$$-\lambda y(x) G_q(y)^2(x,x) = -\lambda a_2(q) y(x) + O(y^3).$$

The coefficient $a_2(q)$ has continuum size $q^{-1/2}$ in three dimensions. Its integral to infinity is divergent; at fixed N it is finite, but grows with the cutoff. This is the tadpole mass correction. Further insertions also produce the logarithmically divergent sunset. These divergent terms are constant modes, and must be incorporated into a running scalar mass, rather than estimated as a small remainder.

Why we project. For a smooth odd force f, define

$$(\Pi f)(y) := f(y) - \mathrm{Df}(0)y, \qquad ((1-\Pi)f)(y) = \mathrm{Df}(0)y.$$

Thus $\Pi^2 = \Pi$, $D(\Pi f)(0) = 0$, and Πf starts at cubic order in the field. Π removes the whole linear jet, and keeps the cubic interaction and higher vertices. Only the constant mode of the linear jet needs a condition at a finite scale; the rest can be integrated from infinity like the vertices. All kernels at zero field are translation invariant, and for such an operator L we write

$$L = \langle L \rangle I + L^\circ, \qquad L1 = \langle L \rangle 1,$$

with $\langle L \rangle$ its constant-mode eigenvalue and L° centred, $L^\circ 1 = 0$. The divergences above are constant modes: the tadpole is a local term, a multiple of the identity, and so is the divergent part of the sunset. The centred part of the linear flow is different: once the local term is subtracted, what remains is a nonlocal kernel whose first spatial moment is integrable at infinite resolution (Section 11.3). So we also use the projection that removes only the scalar part of the linear jet,

$$(\Pi' f)(y) := f(y) - \langle \mathrm{Df}(0) \rangle y = (\Pi f)(y) + (\mathrm{Df}(0))^\circ y.$$

Everything in the range of Π' is integrable at infinite resolution (shown in Section 11.3) and is fixed there by the bare force, whose linear part is the scalar $\mu_N y$; only the scalar mass needs a condition at a finite scale. Within the range of Π' we still split off the centred linear part with Π, since it is measured differently: vertices in rooted norms, the centred kernel by its first spatial moment. We write the force as

$$\bar{\mathcal{F}}_q = U' + M_q y + \ell_q, \qquad M_q = \mu_q I + \Theta_q,$$

with $\Pi\ell_q = \ell_q$, a running scalar mass μ_q and an even, translation-invariant, centred kernel Θ_q. The nonlinear remainder ℓ and the centred kernel Θ are integrated from infinity, where they vanish, and are computed by the same finite iteration; the scalar mass is fixed at a finite reference scale, and the bare counterterm is then an output of the flow. We first establish the size of a loop, then compute the seed and its two corrections.

11.1 Scales and power counting

Two scales govern everything:

$$g_q := \lambda\, q^{-1/2}, \qquad r_q := (q/\lambda)^{1/2}, \qquad \lambda\, r_q^2 = q. \tag{11.1}$$

g_q is the dimensionless coupling at resolution q: in $d=3$ the coupling λ has dimension of mass, and $q^{1/2}$ is the mass of the regulator. It is small at all scales $q \geqslant q_*$ if $g_{q_*} = \lambda\, q_*^{-1/2}$ is small; this is the only large number in the construction, and it is not a physical mass. r_q is the field size at which the nonlinearity is comparable to the regulator: $D^2U(y) = \lambda y^2 \approx q$ when $|y| \approx r_q$. Compare with the size of the free field at resolution q:

$$\mathrm{Var} X_q(x) = \int_{q_0}^{q} a_2 \leqslant C\, q^{1/2},$$

so typical fields have size

$$q^{1/4} = g_q^{1/2} r_q \ll r_q.$$

We measure a k-tensor $T(x_1,\dots,x_k)$ (for instance a **vertex** with k legs, the kernel of the $(k-1)$th field derivative of a force) by its rooted norm

$$s(T) = \max_i \sup_{x_i} \int |T(x_1,\dots,x_k)| \prod_{j\neq i} \mathrm{d}x_j, \tag{11.2}$$

and a force g by

$$\mathsf{S}_k(g) = \sup_{y\in\mathcal{B}_q} s(D^{k-1} g(y)) \tag{11.3}$$

on the field ball

$$\mathcal{B}_q := \big\{ y \in H_N : \|y\|_\infty < 2\, r_q \big\}.$$

The natural size of the k-leg vertex of the loop corrections (recall $U' = DU = \frac{\lambda}{3} y^3$ the bare force, M_q a linear mass term)

$$\ell_q = \bar{\mathcal{F}}_q - U' - M_q y$$

to the bare force is

$$\mathsf{S}_k(\ell_q) \lesssim g_q\, q\, r_q^{2-k}. \tag{11.4}$$

For $k=2$ this says the derivative of the correction force is $g_q = \lambda\, q^{-1/2}$ times the regulator q (while $D^2 U \approx q$ at $|y| \approx r_q$); each extra field derivative costs r_q^{-1}. For $k=4$, $g_q\, q\, r_q^{-2} = \lambda\, g_q$: the four-leg vertex of the corrections is λ times the small coupling. The whole construction is a bookkeeping of (11.4).

The basic loop estimate. The loop $\frac{1}{2}\mathrm{Ctr}_{H^2} D^2 \bar{\mathcal{F}}$ and its derivatives are closed chains

$$H\,(D^{j_1+1}\bar{\mathcal{F}})H \cdots (D^{j_p+1}\bar{\mathcal{F}})H.$$

A closed loop with p vertices, each carrying at least one external leg (vertices without external legs are resummed into H), and $p+1$ propagators H (two of them adjacent, H^2, once the loop is closed) is estimated by rooting one external slot, using two propagators in L^2 (each row has L^2 norm $\leqslant (a_2)^{1/2}$) and the others in operator norm ($\leqslant C/q$):

$$s(\text{loop}) \leqslant C\, a_2\, q^{-(p-1)} \prod_{i=1}^{p} s(T_i) \tag{11.5}$$

Indeed, by cyclicity of the trace we may take the rooted slot x on T_1. Integrating out the other external legs, each T_i, $i \geqslant 2$, is dominated by a kernel $t_i(u,v)$ in its two internal legs whose rows and columns have L^1 norm $\leqslant s(T_i)$, so $\|t_i\|_{2\to 2} \leqslant s(T_i)$ by Schur's test; T_1 with x fixed gives a kernel t_1^x with $\int t_1^x \leqslant s(T_1)$. The rest of the loop is a kernel $|H|R|H|$, where the two propagators next to T_1 are kept apart and R collects the other $p-1$ propagators and $t_2, \dots, t_p$. By Cauchy–Schwarz its entries are bounded by

$$\sup_x \|H(x,\cdot)\|_2^2 \|R\|_{2\to 2} \leqslant C a_2\, (C/q)^{p-1} \prod_{i\geqslant 2} s(T_i),$$

and integrating against t_1^x gives (11.5). We used only that the propagators are symmetric with rows of L^2 norm $\leqslant C a_2^{1/2}$ and of L^1 norm $\leqslant C/q$, which also bounds their operator norm on L^2. For the free resolvent these are $\int C_q(x,z)^2 \mathrm{d}z = a_2$ and $\int C_q(x,z)\mathrm{d}z = q^{-1}$ (Lemma 10.1); for the propagators used below they are (12.3), and Lemma 20.1 of the Supplement.

The vertices of the bare force have

$$s\,(D^{j+2} U) \leqslant C\, q\, r_q^{-j}$$

on the ball ($D^3 U = 2\lambda y$, $D^4 U = 2\lambda$). With $a_2 \leqslant C q^{-1/2}$, a loop with k external legs built from them is $\leqslant C q^{1/2} r_q^{-k}$, and after the integration in q that produces the force $\mathcal{F}$ (which gains a factor q) it has size $q^{3/2} r_q^{-k} = g_q q r_q^{2-k}$: this is the origin of (11.4), the size of one loop. Replacing a bare vertex by a vertex of a correction of relative size ε multiplies the loop by ε (Exercise 11.1). *Every further loop gains one power of g_q.*

11.2 The seed: one loop

Insert the bare force U' in both occurrences of the force on the right-hand side of the Wetterich equation: in the response and in the differentiated vertex. Applying Π gives

$$\Pi[-\lambda y(x) G_s(y)^2(x,x)] = -\lambda y(x)[G_s(y)^2(x,x) - a_2(s)].$$

Since $\partial_s G_s = -G_s^2$ and $\partial_s C_s = -C_s^2$, integration from infinity with zero nonlinear boundary value gives the one-loop seed of Exercise 8.6(b), which we call $\ell^{[1]}$: the superscript counts loops (see the iteration below),

$$\ell_q^{[1]}(y)(x) = \lambda y(x)[G_q(y)(x,x) - C_q(x,x)], \quad \partial_q \ell_q^{[1]}(y)(x) = -\lambda y(x)[G_q(y)^2(x,x) - a_2(q)], \tag{11.6}$$

with $G_q(y) = (K_q + \lambda y^2)^{-1}$. It is odd, and its linear Taylor coefficient at $y=0$ vanishes. Its expansion in powers of the field,

$$\ell_q^{[1]}(y)(x) = \lambda y(x) \sum_{j\geqslant 2} (-1)^{j-1} [C_q (\lambda y^2 C_q)^{j-1}](x,x),$$

is the sum of one-loop diagrams with $2j$ external legs, one of them the output x. The leading term is the bubble

$$-\lambda^2 y(x) \int C_q(x,z)^2 y(z)^2\, \mathrm{d}z,$$

with (use (11.2) and (10.4))

$$s(D^3\ell_q^{[1]}(0)) = 6\lambda^2 \int C_q(x,z)^2 \mathrm{d}z = 6\lambda^2 C_q^2(x,x) = 6\lambda^2 a_2(q) \leqslant C g_q q\, r_q^{-2},$$

as predicted by (11.4).

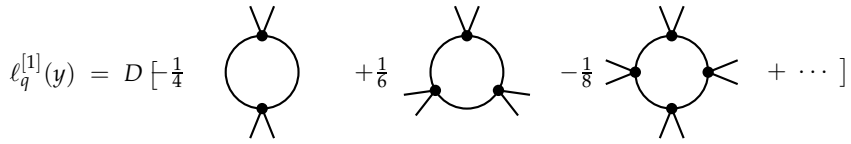


Figure 11.1. The seed (11.6) as one-loop graphs: lines C_q, and a vertex λy^2 with its two external fields at each corner. The j-th ring has $2j$ legs and coefficient $(-1)^{j+1}/(2j)$. Marking one leg of a ring gives its term in the seed force. The series sums to a logarithm and has radius of convergence r_q. The quartic ring is the bubble.

11.3 Corrections and the mass

The seed used only the bare cubic force inside the loop. We now feed the corrected force back into both the response and the vertex. For this calculation first prescribe a trial scalar mass path $(\mu_q)_q$. The two steps then define functions of that path, the corrections $\ell^{[2]}[\mu]$, $\ell^{[3]}[\mu]$ and the centred kernels $\Theta^{[2]}[\mu]$, $\Theta^{[3]}[\mu]$. Substituting them into the scalar mass equation defines a separate fixed-point problem for μ. Thus there are two distinct operations: a finite recursion in the force, followed by a contraction on scalar mass paths. We suppress the argument $[\mu]$ during the calculation. The section proceeds in this order: the splitting of the force equation and the iteration; why the centred kernel is integrable from infinity; the two corrections and their bounds; the scalar mass equation; the defect of the final approximation; and the fixed point for μ. For a linear operator path $M = \mu I + \Theta$ as above we define the *loop map*

$$\mathcal{J}_q[M,\ell](y) := -\frac{1}{2}\mathrm{C}\mathrm{tr}_{R^2} D^2(U'+\ell)(y), \qquad R = (K_q + M_q + D(U'+\ell)(y))^{-1}. \tag{11.7}$$

Splitting the force equation. The exact force solves the force equation (10.10),

$$\partial_q \mathcal{F}_q = -\frac{1}{2}\mathrm{C}\mathrm{tr}_{H_q^{\mathrm{ex}2}} D^2 \mathcal{F}_q,$$

and becomes the bare force

$$D V_N = U' + \mu_N y$$

at $q = \infty$. Write an odd candidate as

$$\mathcal{F}_q = U' + M_q y + \ell_q:$$

the bare cube, a linear part, and a nonlinear remainder without linear Taylor coefficient, $\Pi\ell_q = \ell_q$. Since $\partial_q U' = 0$, $D^2(M_q y) = 0$ and $D\mathcal{F}_q = M_q + D(U' + \ell_q)$, the force equation reads, with the trace map (11.7),

$$(\partial_q M_q) y + \partial_q \ell_q = \mathcal{J}_q[M, \ell_q](y).$$

With the splitting $L = \langle L \rangle I + L^\circ$ of the linear part, the projections Π and $1 - \Pi$ give three equations of different nature:

$$\partial_q \ell_q = \Pi \mathcal{J}_q[M,\ell_q], \qquad \partial_q \Theta_q = (D\mathcal{J}_q[M,\ell_q](0))^\circ, \qquad \partial_q \mu_q = \langle D\mathcal{J}_q[M,\ell_q](0)\rangle.$$

The first is the nonlinear part of the flow. By power counting (11.4) its vertices with $k \geqslant 4$ legs have integrands $O(s^{(1-k)/2})$, integrable at $s = \infty$, so it can be integrated from infinite resolution with the boundary value $\ell_\infty = 0$ required by the bare force:

$$\ell_q = -\int_q^\infty \Pi \mathcal{J}_s[M,\ell_s]\,\mathrm{d}s.$$

This is a fixed-point equation: ℓ appears on both sides, inside the propagator R and in $D^2\ell$. The second, the centred linear part, is integrable at infinity as well (its source is estimated below, in first moment), so Θ is integrated from infinity, with $\Theta_\infty = 0$. The third, the scalar mass, is not integrable at $q=\infty$ uniformly in N, since the tadpole and the sunset diverge (Section 11.4). It is pinned at q_*, as specified in the mass equation (11.9) below, and its limit is the bare mass. In the language of the projections, $\Pi' \mathcal{J} = \Pi \mathcal{J} + (D\mathcal{J}(0))^\circ y$ is the convergent part of the flow, which we approximate by the iteration; the scalar mass is solved exactly and produces the counterterm.

The iteration as Picard steps. Start from $\ell^{[0]} = 0$, so that the superscript counts loops. The first step is taken without the mass: the seed (11.6) obeys $\partial_q \ell_q^{[1]} = \Pi \mathcal{J}_q[0, \ell^{[0]}] = \Pi \mathcal{J}_q[0,0]$ and vanishes at infinity. The linear part of $\mathcal{J}_q[0,0]$ at zero field is the local tadpole, a multiple of the identity, so the first step produces no centred kernel: $\Theta^{[1]} = 0$, and $M^{[1]} = \mu I$. Every later step uses the *level mass*

$$M_q^{[j]} = \mu_q I + \Theta_q^{[j]}, \qquad j \geqslant 1,$$

with the same scalar path at every level. Write $R_{0,q}^{[j]} = (K_q + M_q^{[j]})^{-1}$ for its zero-field response, and

$$\mathfrak{S}_q^{[j]} := D\mathcal{J}_q[M^{[j]}, \ell^{[j]}](0) = -\lambda \mathrm{Tr}\big((R_{0,q}^{[j]})^2\big) I - \tfrac{1}{2} C \mathrm{tr}_{(R_{0,q}^{[j]})^2} D^3 \ell_q^{[j]}(0)$$

for the linear coefficient of the loop map at zero field, the *source* of the linear flow at level j (by oddness; the first term is the tadpole). Each step integrates the flow evaluated at the previous approximation, from infinity; we write $\delta^{[j]} = \ell^{[j]} - \ell^{[j-1]}$ for the increments. Subtracting the seed equation from the nonlinear part gives the equivalent, more useful form

$$\begin{aligned} \ell^{[0]} = 0, \quad \ell_q^{[j+1]} &= \ell_q^{[1]} - \int_q^\infty \Pi(\mathcal{J}_s[M^{[j]}, \ell^{[j]}] - \partial_s \ell_s^{[1]})\, \mathrm{d}s, \\ \Theta^{[1]} = 0, \quad \Theta_q^{[j+1]} &= -\int_q^\infty (\mathfrak{S}_s^{[j]})^\circ \mathrm{d}s, \qquad j = 1,2, \end{aligned} \tag{11.8}$$

so that

$$\partial_q \ell^{[j+1]} = \Pi \mathcal{J}_q[M^{[j]}, \ell^{[j]}], \qquad \partial_q \Theta^{[j+1]} = (\mathfrak{S}_q^{[j]})^\circ :$$

each step inserts the previous approximation, nonlinear correction and centred kernel, into the loop. The integrals run from ∞, where the force must become the bare one (Theorem 8.2), as explained in the introduction to this section.

Why the first spatial moment is the right quantity. For a translation-invariant kernel write $\Theta(z) = \Theta(0,z)$ and

$$v_1(\Theta) = \int d(0,z) |\Theta(z)| \mathrm{d}z$$

for its first spatial moment; the analogous moment $v_1(T)$ of a k-leg tensor is defined in "Following a spatial distance through a loop" below. For an even kernel, centring means $\Theta 1 = 0$, or $\int \Theta(z) \mathrm{d}z = 0$. Thus the diagonal coefficient cancels the total off-diagonal mass. Define $(\sigma_z f)(x) = f(x+z)$ and $\delta_z^2 = \sigma_z + \sigma_{-z} - 2I$. Before taking absolute values, use centring and evenness to write

$$\Theta f = \frac{1}{2} \int \Theta(z) \delta_z^2 f \, \mathrm{d}z, \qquad C_q \Theta = \frac{1}{2} \int \Theta(z) \delta_z^2 C_q \mathrm{d}z.$$

The absolute row norm $\|\Theta\|_{\mathrm{row}} = \int |\Theta(z)| \mathrm{d}z$ discards this cancellation. It would give only $\|C_q \Theta\|_{\mathrm{row}} \leqslant q^{-1} \|\Theta\|_{\mathrm{row}}$, which is not small uniformly in the cutoff. For example, for a lattice step h in a coordinate direction e and $a > 0$, the centred kernel

$$\Theta_h = \frac{a}{2h} (\sigma_{\mathrm{he}} + \sigma_{-\mathrm{he}} - 2I)$$

has $v_1(\Theta_h) = a$ but $\|\Theta_h\|_{\mathrm{row}} = 2a/h$. Its absolute row norm diverges as $h \to 0$, even though its effect after a resolvent remains controlled. This example explains why bounding the bare kernel in absolute value is too strong a requirement.

The resolvent receives the cancellation. The free resolvent smooths translations on the length scale $q^{-1/2}$. Uniformly in the lattice cutoff,

$$\|\delta_z^2 C_q\|_{\mathrm{row}} \leqslant C q^{-1/2} d(0,z).$$

One way to see the scale is to write $C_q = \int_0^\infty \mathrm{e}^{-\mathrm{q}t} p_t \mathrm{d}t$. The heat-kernel translation estimate $\|(\sigma_z - I)p_t\|_1 \leqslant C\, d(0,z) t^{-1/2}$ gives the bound by integration, since $\int_0^\infty \mathrm{e}^{-\mathrm{q}t} t^{-1/2} \mathrm{d}t = \sqrt{\pi} q^{-1/2}$. Insert this estimate into the signed identity above, and only then take absolute values:

$$\|C_q \Theta\|_{\mathrm{row}} \leqslant C q^{-1/2} \int d(0,z) |\Theta(z)| \mathrm{d}z = C\, \eta_q(\Theta),$$

where $\eta_q(\Theta) = q^{-1/2} v_1(\Theta)$. The estimate in the weighted convolution norm used for loops is proved in Lemma 19.3 of the Supplement. Although centring gives a second difference, a bound by $d(0,z)^2$ without a logarithmic loss is not available uniformly at kinetic order two. One distance power is enough, and the scale factor $q^{-1/2}$ supplies the required gain.

From the free resolvent to the loop response. This cancellation remains useful when the field is nonconstant. Put $V_y = \lambda y^2$ and $G = (K_q + V_y)^{-1}$. Since $G = (I - \mathrm{G}\mathrm{V}_y) C_q$,

$$G\Theta = (I - \mathrm{G}\mathrm{V}_y) C_q \Theta, \qquad \|G\Theta\|_{\infty\to\infty} \leqslant 2 \|C_q \Theta\|_{\mathrm{row}}.$$

Indeed, positivity and $\mathrm{G}\mathrm{V}_y 1 = 1 - q\, G1$ imply $\|\mathrm{G}\mathrm{V}_y\|_{\infty\to\infty} \leqslant 1$. For the full response $R = (K_q + M + \mathrm{D}\mathrm{U}' + D\ell)^{-1}$, the Neumann series in $R = (I + G(M + D\ell))^{-1} G$ has bounded norm on the admissible ball. Thus the small insertion is $R\delta M$, not δM on its own:

$$\|R\delta M\|_{\infty\to\infty} \leqslant C \rho_q, \qquad \rho_q = \frac{|\delta\mu_q|}{q} + q^{-1/2} v_1(\delta\Theta_q).$$

Keeping the nonlinear correction fixed while changing M, the resolvent identity gives $\delta R = -R\delta M \hat{R}$, with $\hat{R}$ the response at the mass $M - \delta M$. Consequently its row norm is bounded by $C\rho_q/q$, and its row L^2 norm by $C\rho_q \sqrt{a_2(q)}$. These are the original propagator bounds multiplied by ρ_q, so the marked propagator in a loop gains exactly that relative factor. The weighted version is the comparison in Lemma 20.4.

Why the centred source is integrable. The first-moment bound on $\Theta^{[j+1]}$ is an output of the iteration. To see it, separate its source $\mathfrak{S}_q^{[j]}$ into the local tadpole and the correction vertex:

$$\mathfrak{S}_q^{[j]} = -\lambda \mathrm{Tr}\big((R_{0,q}^{[j]})^2\big) I + E_q, \qquad E_q = -\frac{1}{2} \mathrm{C}\mathrm{tr}_{(R_{0,q}^{[j]})^2} T_q, \quad T_q = D^3 \ell_q^{[j]}(0).$$

Here T_q is a four-leg tensor; E_q and T_q depend on the level, which we do not write. Since all kernels at zero field are translation invariant, write $E_q 1 = e_q 1$. The constant mode is $\langle \mathfrak{S}_q^{[j]} \rangle = -\lambda \mathrm{Tr}\big((R_{0,q}^{[j]})^2\big) + e_q$, so the source of the centred kernel is exactly

$$(\mathfrak{S}_q^{[j]})^\circ = E_q - e_q I.$$

The tadpole cancels completely. More generally, any local term $c_q I$ cancels in this subtraction. The scalar part, including the divergent mass contributions, is the constant mode; only that of the final level enters the mass equation (11.9). Off the diagonal, centring leaves E_q unchanged; it only adjusts the diagonal so that the row sum is zero. Since the distance vanishes on the diagonal,

$$v_1((\mathfrak{S}_q^{[j]})^\circ) = v_1(E_q - e_q I) = v_1(E_q).$$

Thus centring removes the local obstruction, but does not itself create spatial decay. The remaining estimate comes from the first moment of the nonlinear vertex.

The vertex pays for the spatial moment. The weighted comparison through the seed and two corrections, computed below (the four-leg bound after two steps), gives the four-leg vertex bound at every level. There is no circularity: the induction is level by level. $\Theta^{[2]}$ needs only the four-leg vertex of the seed, the bubble, and $\Theta^{[3]}$ only that of $\ell^{[2]}$, which is computed with $M^{[1]}=\mu I$ and no centred kernel. The bound is

$$s(T_q)+\sqrt{q}\,v_1(T_q)\leqslant C g_q q\, r_q^{-2}=C\lambda^2 q^{-1/2}.$$

In particular $v_1(T_q)\leqslant C\lambda^2 q^{-1}$. This is the weighted vertex bound in Proposition 11.2; it follows from the weighted loop estimate of Lemma 20.1 of the Supplement. The two uncontracted legs are the two kernel arguments of E, so

$$E_q(x,y)=-\frac{1}{2}\int R_{0,q}^2(u,v)T_q(x,y,u,v)\,\mathrm{d}u\mathrm{d}v.$$

Cauchy–Schwarz and the row L^2 bound on the response give $\sup_{u,v}|R_{0,q}^2(u,v)|\leqslant C\,a_2(q)\leqslant Cq^{-1/2}$. Keeping the distance $d(x,y)$ in the vertex before integrating its other legs yields

$$v_1(E_q)\leqslant Cq^{-1/2}v_1(T_q)\leqslant C\lambda^2 q^{-3/2}.$$

The response contraction supplies $q^{-1/2}$, while the within-vertex moment supplies $\lambda^2 q^{-1}$. A rooted bound without the vertex moment would not control this distance.

Integrating from infinity. The centred kernel of the next level therefore satisfies

$$v_1(\Theta_q^{[j+1]})\leqslant\int_q^\infty v_1((\mathfrak{S}_s^{[j]})^\circ)\mathrm{d}s\leqslant C\lambda^2\int_q^\infty s^{-3/2}\mathrm{d}s=2C\lambda^2 q^{-1/2}.$$

This proves convergence of the integral in first moment and $v_1(\Theta_q^{[j+1]})\to 0$, for every admissible trial scalar path and uniformly in N; in particular $\eta_q(\Theta^{[2]})\leqslant C g_q^2$. The same argument applied to the difference of consecutive sources, which inserts $\delta^{[2]}$ and $\Theta^{[2]}$ into the loop, gains one more factor g: $\eta_q(\Theta^{[3]}-\Theta^{[2]})\leqslant C g_q^3$. This convergence concerns the centred kernel in first moment; it does not assert a cutoff-uniform bound on its absolute row norm or on the bare scalar mass. The source $(\mathfrak{S}^{[j]})^\circ$ itself, by contrast, does have a cutoff-uniform row norm: it is a contraction of a four-leg vertex, bounded in a rooted norm, against the bounded kernel $(R_{0,q}^{[j]})^2$. This is what makes the linear defect below small in the row norm.

Computing the first correction. To see what is inserted at each step, put

$$R_s^{[j]}(y)=(K_s+M_s^{[j]}+\mathrm{DU}'(y)+D\ell_s^{[j]}(y))^{-1},\quad \delta^{[j]}=\ell^{[j]}-\ell^{[j-1]}.$$

Here $j=1,2,3$; since $\ell^{[0]}=0$, the first increment $\delta^{[1]}=\ell^{[1]}$ is the seed. For the first correction, subtract the bare loop from the loop containing the seed. Suppressing the field argument, this gives exactly

$$\delta_q^{[2]}=\frac{1}{2}\int_q^\infty \Pi\Big[\mathrm{Ctr}_{(R_s^{[1]})^2-G_s^2}D^2U'+\mathrm{Ctr}_{(R_s^{[1]})^2}D^2\ell_s^{[1]}\Big]\mathrm{d}s.$$

The first term changes the propagators; the second changes the vertex. The resolvent identity makes the extra insertion explicit:

$$R^{[1]}-G=-R^{[1]}(\mu+D\ell^{[1]})G.$$

Both μ/q and $D\ell^{[1]}/q$ have size $O(g_q)$ on the ball. Applying the loop estimate to either term therefore adds one power of g to the one-loop seed. For the four-leg vertex the calculation is

$$\mathsf{S}_4(\delta_q^{[2]})\lesssim\int_q^\infty g_s s^{1/2}r_s^{-4}\mathrm{d}s=\lambda^3\int_q^\infty s^{-2}\mathrm{d}s=\lambda^3 q^{-1}.$$

Thus $\ell^{[2]} = \ell^{[1]} + \delta^{[2]}$ contains the seed of size λg_q and a first correction of size λg_q^2 in this vertex.

Remark 11.1. (**Why the corrections also enter the propagators**) The loop map (11.7) is the right-hand side of the exact force equation, whose propagator is the response $(K_q + D\mathcal{F})^{-1}$ of the force itself. So ℓ enters $\mathcal{J}_q[M, \ell]$ twice, in the vertex $D^2\ell$ and in the lines through $D\ell$, and the iteration (11.8) consists of Picard steps for this equation, with both evaluated at the previous approximation. This cannot be dropped. The defect of the final force (Proposition 11.2) measures the force equation at the approximate force, so its loop has the lines of $\ell^{[3]}$. Had the corrections been computed with the lines frozen at G_s, the defect would keep the leading term $\frac{1}{2}\Pi\mathrm{Ctr}_{(R^{[3]})^2 - G^2} D^2 U'$. By the resolvent identity $R^{[3]} - G = -R^{[3]}(M^{[3]} + D\ell^{[3]})G$, and since μ/q and $D\ell^{[3]}/q$ are $O(g_q)$ on the ball, while $\Theta^{[3]}$ is smaller still once it passes through a resolvent ($\eta_q(\Theta^{[3]}) \lesssim g_q^2$), this term is as large as the integrand of $\delta^{[2]}$: its four-leg coefficient is of order $\lambda^3 q^{-2}$, instead of $\lambda^5 q^{-3}$ in (11.14). The defect would never improve beyond one power of g over the seed. In graphs (Figure 11.2), a correction inserted into a line (a self-energy) and one inserted as a vertex give loops with the same number of loops and the same power counting, and an expansion correct to a given order must contain both. Finally, the lines are resummed rather than expanded: $\mathrm{DU}' = \lambda y^2$ stays in $G_q(y) = (K_q + \lambda y^2)^{-1} \leqslant C_q$, which makes the loop estimates uniform in the field, and the mass M resums the tadpoles. Adding $D\ell$, which is small on the ball, preserves the coercivity of $K_q + D\mathcal{F}$ and costs nothing.

Computing the second correction. Subtract the first two Picard equations, keeping the same scalar mass path. This yields

$$\delta_q^{[3]} = \frac{1}{2}\int_q^\infty \Pi\big[\mathrm{Ctr}_{(R_s^{[2]})^2 - (R_s^{[1]})^2} D^2(U' + \ell_s^{[1]}) + \mathrm{Ctr}_{(R_s^{[2]})^2} D^2 \delta_s^{[2]}\big]\mathrm{d}s.$$

Now the marked insertion is the first correction itself, nonlinear and centred:

$$R^{[2]} - R^{[1]} = -R^{[2]}(\Theta^{[2]} + D\delta^{[2]})R^{[1]}.$$

For noncommuting operators one uses

$$A^2 - B^2 = A(A - B) + (A - B)B$$

to split the difference of squared propagators in these formulas. A loop with this insertion gains another power of g; the centred kernel enters only through its first moment, $\eta_q(\Theta^{[2]}) \leqslant C g_q^2$, which the resolvent receives as explained above. This gives

$$\mathsf{S}_4(\delta_q^{[3]}) \lesssim \int_q^\infty g_s^2 s^{1/2} r_s^{-4}\mathrm{d}s = \lambda^4 \int_q^\infty s^{-5/2}\mathrm{d}s = \frac{2}{3}\lambda^4 q^{-3/2}.$$

The second correction is of size λg_q^3 in the four-leg vertex. These calculations also require higher vertices to control the differentiated loops; their precise bounds and the derivative count are given in Proposition 11.2 below.

Following a spatial distance through a loop. The estimates just computed also propagate a first spatial moment. For a symmetric k-leg tensor define

$$v_1(T) = \max_{i,a<b} \sup_{x_i} \int d(x_a, x_b)|T(x_1, \dots, x_k)| \prod_{j \neq i} \mathrm{d}x_j, \quad W_q(T) = s(T) + \sqrt{q}\, v_1(T).$$

The moment is needed only at zero field, where the vertices and propagators are translation invariant. Mark the two external legs whose distance is being measured. If they lie in one vertex, charge the distance to that vertex's first moment. Otherwise connect them along the loop. The triangle inequality bounds their distance by the sum of displacements inside vertices and along propagator edges. Each term is estimated with a weight on the corresponding vertex or edge.

For an edge charge use the weighted convolution bounds

$$\int (1+\sqrt{q}d(0,z))|H(z)|\mathrm{d}z \lesssim q^{-1}, \quad \int (1+\sqrt{q}d(0,z))|H(z)|^2\mathrm{d}z \lesssim q^{-1/2}.$$

Cutting the loop into two chains, use one inverse in each weighted L^2 norm and the remaining inverses in the weighted L^1 norm. For a loop $\mathcal{Z}$ with p vertices and $p+1$ inverse factors this gives

$$W_q(\mathcal{Z}) \leqslant C_p q^{-1/2} q^{-(p-1)} \prod_{i=1}^{p} W_q(T_i).$$

This is Lemma 20.1 of the Supplement. It has the same scale powers as the unweighted loop bound: the factor $\sqrt{q}$ makes a distance of size $q^{-1/2}$ dimensionless. Distances inside a nonlocal vertex must be paid for by that vertex; a propagator bound alone does not control them.

Weighted comparisons and the scale integral. Set $T^{[j]}_{k,q} = \mathrm{D}^{k-1}\ell^{[j]}_q(0)$. If a difference of vertices has relative size ε_s in the weighted bounds through $k+2$ legs, telescope the loop difference onto one changed vertex or one changed inverse. The same distance argument works with this marked factor, and gives

$$W_s(\mathrm{D}^{k-1}(\mathcal{T}_s[M,\ell] - \mathcal{T}_s[M,\hat{\ell}])(0)) \lesssim \varepsilon_s s^{1/2} r_s^{-k}.$$

For a changed inverse, its weighted bounds gain the same relative factor by the resolvent identity. Changes of the level mass are marked insertions too: by the scalar μ in the first comparison, of relative size $|\mu|/q \leqslant C g_q$, and by the centred kernel $\Theta^{[2]}$ in the second, controlled by the centred-kernel estimate above. The projection Π subtracts only a linear force: it does not change any k-leg tensor with $k \geqslant 4$.

Most importantly, an integral from q to infinity is measured with the weight at q, not at the running scale s. Since $\sqrt{q} \leqslant \sqrt{s}$,

$$W_q\Big(\int_q^\infty A_s \mathrm{d}s\Big) \leqslant \int_q^\infty (s(A_s) + \sqrt{q}v_1(A_s))\mathrm{d}s \leqslant \int_q^\infty W_s(A_s)\mathrm{d}s.$$

Thus integrating costs no additional spatial moment. The unweighted supremum over fields is propagated at the same time, because $\mathcal{B}_q \subseteq \mathcal{B}_s$ for $s \geqslant q$. These are the two parts of the norm $\mathcal{N}_{k,q}$ used in Proposition 11.2.

The four-leg bound after two steps. At zero field the seed's four-leg vertex is the bubble: its spatial kernel is built from $\lambda^2 C_q(z)^2$ and local identifications of its legs. Hence

$$W_q(T^{[1]}_{4,q}) \lesssim \lambda^2 \int (1+\sqrt{q}d(0,z))C_q(z)^2\mathrm{d}z \lesssim \lambda^2 q^{-1/2}.$$

Higher seed vertices obey the corresponding weighted bounds through ten legs, by the same cycle estimate. The first loop comparison has $\varepsilon_s = O(g_s)$ from the seed and the admissible mass insertion. The second has $\varepsilon_s = O(g_s^2)$ from the first correction and the centred kernel $\Theta^{[2]}$, with the same scalar mass. Applying the preceding integral estimate at $k=4$ yields

$$W_q(T^{[2]}_{4,q} - T^{[1]}_{4,q}) \lesssim \int_q^\infty g_s s^{1/2} r_s^{-4}\mathrm{d}s = \lambda^3 q^{-1},$$

$$W_q(T^{[3]}_{4,q} - T^{[2]}_{4,q}) \lesssim \int_q^\infty g_s^2 s^{1/2} r_s^{-4}\mathrm{d}s = \frac{2}{3}\lambda^4 q^{-3/2}.$$

The derivative budgets are $10 \to 8 \to 6$ legs, so both comparisons have the higher vertices they require. Summing the seed and the two increments, with $T_q = T^{[3]}_{4,q}$, gives

$$s(T_q) + \sqrt{q}v_1(T_q) \lesssim \lambda^2 q^{-1/2}(1 + g_q + g_q^2) \lesssim \lambda^2 q^{-1/2}.$$

In particular $v_1(T_q) \lesssim \lambda^2 q^{-1}$. This is the spatial input used below to integrate the centred kernels. The statement holds for each admissible trial scalar path: the finite recursion propagates the vertex moment and the first moments of $\Theta^{[2]}$ and $\Theta^{[3]}$.

The scalar mass. The scalar part of the linear term is not truncated at two correction steps. Instead, its flow is imposed exactly for the final approximation by a separate fixed-point equation for μ. The linear part of the flow at $y = 0$ is, by oddness,

$$D\widetilde{\mathcal{J}}_q(0) = -\frac{1}{2}\mathrm{Ctr}_{R_0^2} D^3 \widetilde{\mathcal{F}}^o(0),$$

where $R_{0,q} = (K_q + M_q)^{-1}$. Requiring that μ solves the scalar part of this flow exactly gives the mass equation

$$\partial_q \mu_q = \beta_q := \langle \mathfrak{S}_q^{[3]} \rangle, \qquad \mathfrak{S}_q^{[3]} = -\lambda \mathrm{Tr}(R_{0,q}^2)\, I - \frac{1}{2}\mathrm{Ctr}_{R_{0,q}^2} D^3 \ell_q^{[3]}(0), \tag{11.9}$$

with the boundary condition

$$\mu_{q_*} = b_*.$$

The running mass is pinned at the auxiliary scale q_*, at a value b_* with $|b_*| \leqslant B_0 \lambda q_*^{1/2}$. The centred part of $\mathfrak{S}^{[3]}$ is not imposed: the kernel Θ of the final approximation is the one produced by the iteration, from the source of the previous level.

Why we stop at the second correction. Define the bounded-field approximation by

$$\widetilde{\mathcal{F}}_q^o(y) = U'(y) + M_q y + \ell_q^{[3]}(y), \qquad M_q := M_q^{[3]} = \mu_q I + \Theta_q^{[3]}. \tag{11.10}$$

From now on $M = M^{[3]}$ and $\Theta = \Theta^{[3]}$ denote the linear part of this final approximation.

Choose the scalar mass to solve the scalar part of the linear flow for this final approximation, as in (11.9). Since $\partial_q \ell^{[3]} = \Pi \widetilde{\mathcal{J}}_q[M^{[2]}, \ell^{[2]}]$ and $\partial_q \Theta^{[3]} = (\mathfrak{S}_q^{[2]})^\circ$, and since $\Pi' f = \Pi f + (\mathrm{Df}(0))^\circ y$, its defect is exactly

$$\mathcal{D}_q^o = \Pi'(\widetilde{\mathcal{J}}_q[M^{[2]}, \ell^{[2]}] - \widetilde{\mathcal{J}}_q[M^{[3]}, \ell^{[3]}]):$$

the nonlinear and the centred linear part of a loop difference, the scalar linear part vanishing by the mass equation. The centred linear part is there for the same reason as the nonlinear one: $\Theta^{[3]}$ is built from the source of level 2, while the exact flow would need the source of level 3. This is the price of not solving for Θ exactly, the same price already paid for ℓ. The defect is one loop with an insertion of $\delta^{[3]}$ and of $\Theta^{[3]} - \Theta^{[2]}$. There is no scale integration in the defect, so

$$\mathsf{S}_4(\mathcal{D}_q^o) \lesssim g_q^3 q^{1/2} r_q^{-4} = \lambda^5 q^{-3}, \qquad \|\mathcal{E}_q^c\|_{\mathrm{row}} + q^{1/2} v_1(\mathcal{E}_q^c) \lesssim g_q^4,$$

where $\mathcal{E}_q^c = D\mathcal{D}_q^o(0) = (\mathfrak{S}_q^{[2]} - \mathfrak{S}_q^{[3]})^\circ$ is the centred linear part. The tadpoles, being local, cancel in the centred part. What remains contracts the four-leg vertex of $\delta^{[3]}$ with $R_{0,q}^2$, and the four-leg vertex of $\ell^{[2]}$ with the difference of the squared responses caused by $\Theta^{[3]} - \Theta^{[2]}$. Both are contractions of rooted tensors against bounded kernels, so their row norm is controlled, as for the centred source above; the first moment stays in the vertex. The backward equation uses only the row norm, as an L^∞ operator bound; the first moment is needed only for the continuum limit. In short: Θ is not the exact centred flow, so the final force has a linear defect of relative size g_q^4, and it is harmless because on the ball it has the same size as the cubic defect.

To understand why this is enough, use the backward power count from Section 11.5. On the ball, $\mathcal{D} = O(\mathsf{S}_4(\mathcal{D}) r^3 + \|\mathcal{E}^c\|_{\mathrm{row}} r)$, and after two steps both terms are of size $\lambda^{7/2} q^{-3/2}$; multiplication by H costs q^{-1}, and backward transport from s to q costs about s/q. After only the first correction $\mathsf{S}_4(\mathcal{D})$ would be $\lambda^4 s^{-5/2}$, producing the divergent source integral

$$\lambda^{5/2} q^{-1} \int_q^\infty s^{-1} \mathrm{d}s.$$

After the second correction the corresponding bound is

$$\frac{\lambda^{7/2}}{q}\int_q^\infty s^{-3/2}\mathrm{d}s = 2\lambda^{7/2}q^{-3/2}.$$

Two corrections beyond the one-loop seed are therefore sufficient for this bounded-field source estimate; one is borderline. This explains the depth of the construction, rather than asserting convergence of an infinite Picard iteration. Each step consumes two field derivatives. The rigorous backward estimates, including the terminal condition and the large-field contribution, are proved in Lecture 7.

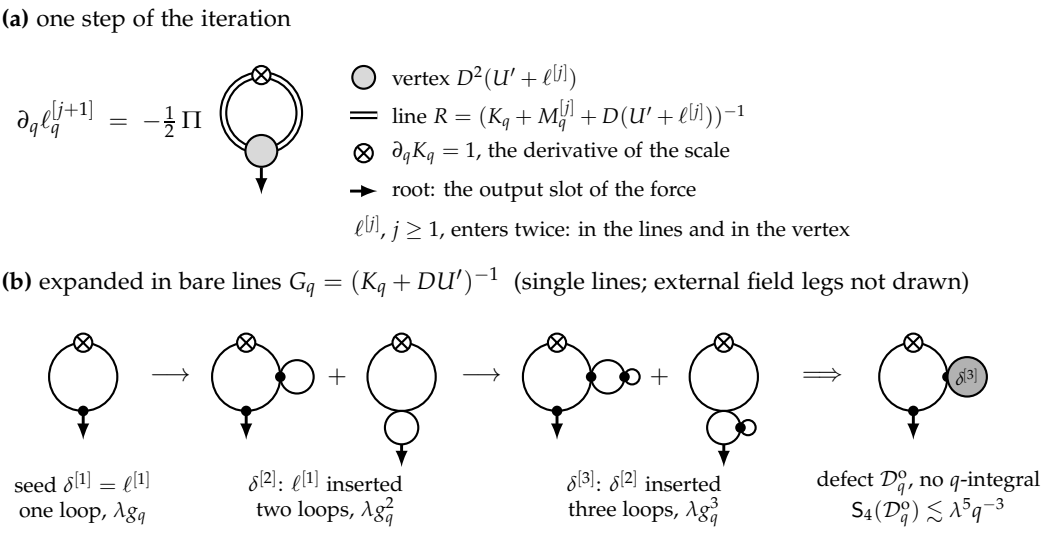


Figure 11.2. The iteration (11.8). (a) One step: the loop map (11.7) at the previous approximation $\ell^{[j]}$, which enters both the propagator and the vertex. (b) The same steps expanded in the bare propagator G_q: each step inserts the previous increment $\delta^{[j]} = \ell^{[j]} - \ell^{[j-1]}$ into the loop, on a line or as the vertex, and gains one loop and one factor g_q, as in (11.13). After two steps the defect is one loop with $\delta^{[3]}$ and $\Theta^{[3]} - \Theta^{[2]}$ inserted, projected by Π', and no scale integral; this gives (11.14) and makes the source integrable in the backward equation. Insertions of the level masses $M_q^{[j]}$ on the lines are not drawn ($M^{[0]} = 0$: the first step is massless).

Closing the mass path. The notation $\beta_q[\mu]$ includes the dependence of the final approximation on the whole trial path. More explicitly, for any admissible scalar path μ first compute the two steps of the iteration, corrections and centred kernels, and set

$$\beta_q[\mu] = \langle D\widehat{\mathcal{J}}_q[M^{[3]}[\mu], \ell^{[3]}[\mu]](0)\rangle.$$

Integrate it from q_* to define a new scalar path

$$\mathcal{A}[\mu]_q = b_* + \int_{q_*}^q \beta_s[\mu]\mathrm{d}s.$$

The desired mass solves $\mu = \mathcal{A}[\mu]$. At a fixed point, $\partial_q \mu_q = \beta_q[\mu]$ and $\mu_{q_*} = b_*$. This is a fixed point on scalar paths over $[q_*, \infty)$, rather than an ordinary initial-value equation: the corrections and the centred kernels at q use the trial path at later scales. It is the only fixed point we actually solve: the exact equations for ℓ and Θ are replaced by two Picard steps, and the centred kernels are explicit outputs of them. The unknown of the fixed point is a scalar function of q, not an operator-valued path.

Two nonlinear steps, one scalar fixed point. For example, start with $\mu_q^{(0)} = b_*$ and repeat

$$\mu^{(n)} \longmapsto (\ell^{[2]}, \Theta^{[2]})[\mu^{(n)}] \longmapsto (\ell^{[3]}, \Theta^{[3]})[\mu^{(n)}] \longmapsto \beta[\mu^{(n)}] \longmapsto \mu^{(n+1)} = \mathcal{A}[\mu^{(n)}].$$

Every evaluation starts again from the same seed and uses precisely two steps; increasing n does not increase their depth. On the admissible ball, use the weighted path norm

$$\|\mu\|_* = \sup_{q \geqslant q_*} \frac{|\mu_q|}{\lambda \sqrt{q}}.$$

Where the small factor comes from. Compare two admissible scalar paths $\mu, \hat{\mu}$ with the same boundary value b_*. Write $d = \|\mu - \hat{\mu}\|_*$; δ denotes the corresponding difference of every output, including the level masses $\delta M^{[j]} = \delta\mu I + \delta\Theta^{[j]}$. In a resolvent, the mass difference is a marked insertion. For the response at level j, the exact identity is

$$R^{[j]}[\mu] - R^{[j]}[\hat{\mu}] = -R^{[j]}[\mu](\delta M^{[j]} + D\delta\ell^{[j]})R^{[j]}[\hat{\mu}].$$

The scalar insertion relative to the regulator obeys $|\delta\mu_q|/q \leqslant g_q d$. The centred kernels are outputs of the iteration, so their differences are computed level by level: the differences of the centred sources obey the moment bound displayed below, and integrating them from infinity gives $q^{-1/2} v_1(\delta\Theta_q^{[j]}) \leqslant C g_q^3 d$. The centred-kernel estimate uses only this first spatial moment; an absolute row norm is not needed. Thus the centred part contributes g_q^3, while the scalar part contributes g_q: the factor comes from cancellation followed by resolvent smoothing, not from small absolute mass of the centred kernel. These are the resolvent comparisons in the proof of Lemma 20.4 of the Supplement. Applying the loop comparison at each of the two fixed levels gives, in the norms of Proposition 11.2,

$$\mathcal{N}_{k,q}(\delta\ell^{[j]}) \leqslant C g_q^2 q\, r_q^{2-k} d, \qquad j = 2,3, \quad 4 \leqslant k \leqslant 12 - 2j.$$

This compares the same level at different scalar paths; it is distinct from the difference between consecutive nonlinear levels. At both levels $j = 2,3$ the path differences of the corrections have relative size g^2. Contracting their four-leg vertices in the sources, and also varying the propagators there, yields for the scalar source of the mass equation, and for the centred sources of the iteration,

$$|\delta\beta_q| \leqslant C g_q^2 d = C\lambda^2 q^{-1} d, \qquad v_1(\delta(\mathfrak{S}_q^{[j]})^\circ) \leqslant C\lambda^3 q^{-2} d.$$

For the scalar bound, a one-loop source of size g_q gains the relative insertion $g_q d$. In the centred bound the local quartic contributes only to the scalar; the spatial moment stays in the nonlocal four-leg tensor. Its source has size $\lambda^2 q^{-3/2}$ and gains the same extra factor. The precise comparisons are in the proof of Proposition 20.6.

Integrating and normalising the differences. Since the two paths have the same value b_*, it cancels in the scalar update:

$$|\delta\mu_q^{\mathrm{new}}| \leqslant C\lambda^2 d \int_{q_*}^{q} \frac{\mathrm{d}s}{s} = C\lambda^2 \log(q/q_*) d.$$

Divide by its path weight $\lambda\sqrt{q}$ and set $x = q/q_* \geqslant 1$:

$$\frac{|\delta\mu_q^{\mathrm{new}}|}{\lambda\sqrt{q}} \leqslant C g_{q_*} \frac{\log x}{\sqrt{x}} d \leqslant \frac{2C}{\mathrm{e}} g_{q_*} d.$$

Here $\sup_{x \geqslant 1} \log x/\sqrt{x} = 2/\mathrm{e}$. This proves

$$\|\mathcal{A}[\mu] - \mathcal{A}[\hat{\mu}]\|_* \leqslant C g_{q_*} \|\mu - \hat{\mu}\|_*.$$

The centred kernels are not part of the unknown of the fixed point: their variation is already contained in $\delta\beta$.

The individual source bounds also show that $\mathcal{A}$ preserves a fixed admissible ball. Choose its radius first, then take q_* large enough for the resolvent bounds and $C g_{q_*} < 1/2$. Banach's theorem gives the unique scalar mass path on the whole half-line, uniformly in N. The scalar logarithm causes no loss: the weight $\sqrt{q}$ absorbs it, leaving precisely g_{q_*}.

Why the outer contraction loses no more derivatives. The derivative loss belongs to applying the nonlinear loop map, which requires a $(k+2)$-leg vertex to control a k-leg output. One evaluation of $\mathcal{A}$ always has the same finite budget:

$$\ell^{[1]}\text{: 10 legs} \longrightarrow \ell^{[2]}\text{: 8 legs} \longrightarrow \ell^{[3]}\text{: 6 legs} \longrightarrow \text{defect: 4 legs.}$$

For a force, a k-leg vertex is its $(k-1)$th field derivative. The mass source itself uses only the four-leg vertex of $\ell^{[3]}$, and the centred sources those of $\ell^{[1]}$ and $\ell^{[2]}$. A difference of scalar paths adds the marked insertions $\delta M^{[j]} = \delta\mu I + \delta\Theta^{[j]}$ in the resolvent identity; these operators are independent of the field, so $D_y \delta M^{[j]} = 0$. Comparing the two finite constructions therefore uses the same budgets as constructing them. This is a Lipschitz comparison in the mass parameter, not an extra application of the nonlinear loop map.

Crucially, $\mathcal{A}$ returns a scalar path, not the final force correction as a new seed. At outer step $n+1$ we restart from the original seed with the new path $\mu^{(n+1)}$; we do not apply a further loop step to $\ell^{[3]}[\mu^{(n)}]$. The contraction acts on the fixed complete space of scalar paths. The finite Lipschitz estimates above then give convergence of the corrections and of the centred kernels in their respective fixed norms. At the limit the scalar part of the linear flow is exact for $\mathcal{F}^o$, while its defect, nonlinear and centred linear, remains the difference of the last two levels.

The bare mass is then

$$\mu_N = \lim_{q\to\infty} \mu_q = b_* + \int_{q_*}^{\infty} \beta_q \, \mathrm{d}q, \tag{11.11}$$

and it is this number that enters the Gibbs measure (10.5).

Proposition 11.2. (The coefficient construction) *For $q_* \geqslant \max(1, q_0)$ large enough, depending on λ and B_0 but not on N, and $|b_*| \leqslant B_0 \lambda q_*^{1/2}$, the system (11.8)–(11.9) has a unique scalar mass path in a ball, and, with $M_q = \mu_q I + \Theta_q^{[3]}$ as in (11.10),*

$$|\mu_q| \leqslant C\lambda\sqrt{q}, \qquad v_1(\Theta_q^{[j]}) \leqslant C\lambda^2 q^{-1/2}, \qquad \|\partial_q M_q\|_{\mathrm{row}} \leqslant C g_q, \tag{11.12}$$

where $v_1(\Theta) = \int d(0,z)\,|\Theta(0,z)|\mathrm{d}z$; moreover $\eta_q(\Theta^{[2]}) \leqslant C g_q^2$ and $\eta_q(\Theta^{[3]} - \Theta^{[2]}) \leqslant C g_q^3$. The increments, the seed $\delta^{[1]} = \ell^{[1]}$ included, obey

$$\mathcal{N}_{k,q}(\ell^{[j]} - \ell^{[j-1]}) \leqslant C_k \, g_q^j \, q \, r_q^{2-k}, \qquad 4 \leqslant k \leqslant 12 - 2j, \quad j = 1,2,3, \tag{11.13}$$

where $\mathcal{N}_{k,q}(f) = \mathsf{S}_k(f) + \sqrt{q}\; v_1(D^{k-1} f(0))$, and for a k-tensor

$$v_1(T) = \max_{i, a<b} \sup_{x_i} \int d(x_a, x_b)|T| \prod_{j\neq i} \mathrm{d}x_j.$$

The complete defect of $\mathcal{F}^{\mathrm{o}}$ on the ball is

$$\mathcal{D}_q^{\mathrm{o}} = \Pi'\,(\mathcal{T}_q[M^{[2]}, \ell^{[2]}] - \mathcal{T}_q[M^{[3]}, \ell^{[3]}]),$$

and

$$\mathsf{S}_4(\mathcal{D}_q^{\mathrm{o}}) \leqslant C\lambda^5 q^{-3}, \qquad \|\mathcal{E}_q^c\|_{\mathrm{row}} + q^{1/2} v_1(\mathcal{E}_q^c) \leqslant C g_q^4, \tag{11.14}$$

where $\mathcal{E}_q^c = D\mathcal{D}_q^{\mathrm{o}}(0)$ is the linear part of the defect, a centred kernel. At fixed N the bare mass exists, $|\mu_N - b_*| \lesssim \lambda \mathrm{Tr} C_{q_*} \lesssim \lambda N$, and $|\mu_N - \mu_q| \leqslant C\lambda N^3/q$, $\|\Theta_q^{[3]}\|_{\mathrm{row}} \leqslant C N \lambda^2 q^{-1/2} \to 0$ as $q \to \infty$.

Idea of the proof (complete proof: Proposition 20.6 of the Supplement). (a) *Loop Lipschitz estimate.* If two corrections $\ell, \hat{\ell}$ obey the individual bounds (11.4) up to order $k+2$ and their difference obeys them with g_q replaced by ε_q, then $\mathcal{N}_k(\mathcal{T}[M,\ell]-\mathcal{T}[M,\hat{\ell}]) \leqslant C\,\varepsilon_q\, q^{1/2} r_q^{-k}$. Expand D^{k-1} of the loop force into loops; in each, telescope the difference onto one marked vertex or propagator and apply (11.5). (b) *Integration.* Each step gains one g; the integrand of (11.8), after subtracting the seed, is $O(\lambda^{1+k/2} s^{-k/2})$ in the k-leg vertex, and that of the increment $\ell^{[j+1]}-\ell^{[j]}$ is $O(\lambda^{1+k/2} s^{-k/2} g_s^{j-1})$, $j \geqslant 1$, integrable at $s=\infty$ for $k \geqslant 4$. The low jets have been removed, so the lower derivatives are controlled by Taylor's formula from the four-leg vertex. (c) *Scalar mass path.* Given μ in the ball, the right side of (11.9) is computed from the two steps $(\ell^{[2]}, \Theta^{[2]})[\mu]$ and $(\ell^{[3]}, \Theta^{[3]})[\mu]$. The boundary-integrated map $\mathcal{A}$ defined above is a contraction for large q_*: differences gain a factor g_{q_*} (for μ after integrating from q_*, using $\sup_x \log x / \sqrt{x} < \infty$). (d) *Defect.* The mass equation supplies exactly the scalar linear jet of the flow, and $\partial_q \ell^{[3]} = \Pi\,\mathcal{T}[M^{[2]}, \ell^{[2]}]$, $\partial_q \Theta^{[3]} = (D\mathcal{T}[M^{[2]}, \ell^{[2]}](0))^\circ$, so the defect is the loop difference between the last two approximations, of order g^3: by (a) with $\varepsilon_q = g_q^3$, $\mathsf{S}_4(\mathcal{D}^\circ) \leqslant C g_q^3 q^{1/2} r_q^{-4} = C\lambda^5 q^{-3}$. Its centred linear part has no tadpole contribution, the tadpole being local; it contracts the four-leg vertex of $\delta^{[3]}$ with $R^2_{0,q}$, whose supremum is $C q^{-1/2}$, and the four-leg vertex of $\ell^{[2]}$ with the change of $R^2_{0,q}$ caused by $\Theta^{[3]}-\Theta^{[2]}$: both are $O(g_q^4)$ in the row norm. □

Two technical points are hidden in this sketch. First, the loop estimate (a) needs more derivatives than it controls: the k-leg vertex of the loop involves vertices with $k+2$ legs. Ten legs of the seed leave eight after one step and six after two; this is why the number of steps must be finite and fixed in advance (an infinite iteration loses all derivatives). Second, the nonlocal kernel Θ_q must be measured in a first spatial moment v_1, not in a second one: the estimate $\|\delta_z^2 C_q\|_{\mathrm{row}} \lesssim d(0,z)^2$, which a second moment would require, fails by a logarithm, and one uses $\|\delta_z^2 C_q\|_{\mathrm{row}} \lesssim q^{-1/2} d(0,z)$ instead (Lemma 19.3 of the Supplement). Distances inside a vertex must be paid for by the vertex itself ("The vertex pays for the spatial moment"), which is why $\mathcal{N}_k$ contains a spatial moment at $y=0$.

11.4 Two mass renormalisations

The bare mass μ_N diverges as $N \to \infty$. Its two divergent parts are the two divergent self-energy diagrams of Appendix A.2 of Lecture 5.

- *The tadpole.* The first term of (11.9) integrates to

$$-\lambda \int_{q_*}^{\infty} \mathrm{Tr} R^2_{0,q}\, \mathrm{d}q \approx -\lambda \mathrm{Tr} C \sim -\lambda N$$

  (up to a term bounded uniformly in N). This is Wick ordering: $\frac{\lambda}{12}\varphi^4 - \frac{1}{2}\lambda c\,\varphi^2$ agrees, up to a constant, with $\frac{\lambda}{12} H_4(\varphi; c)$, with $c = C(x,x)$ ((A.5) of Lecture 5).

- *The sunset.* The second term contracts the bubble contained in $D^3\ell^{[3]}(0)$ (the cubic coefficient of the seed force) with R_0^2, and integrating in q produces the two-loop self-energy, which diverges like

$$\lambda^2 \int_{|z|>1/N} |z|^{-3} \mathrm{d}z \sim \lambda^2 \log N.$$

  This is the sunset counterterm $\gamma_T \sim \log T$ of (A.7) of Lecture 5: with $\gamma_T \int H_2 = \gamma_T \int \varphi^2 + \mathrm{const}$, the sunset part of μ_N is

$$2\gamma_T = \frac{2}{3}\lambda^2 \int C^3 \approx \frac{\lambda^2}{24\pi^2} \log N,$$

  positive. (The double-tadpole logarithms in the two terms of (11.9), the bubble with a tadpole insertion and the mass insertion in $\mathrm{Tr} R^2_{0,q}$, cancel each other.)

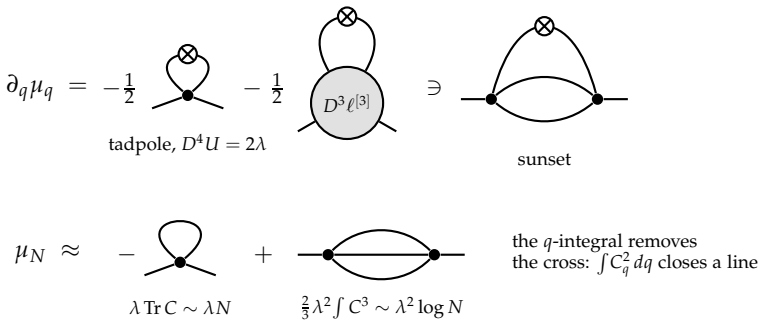


Figure 11.3. The mass equation (11.9), the constant mode of the two diagrams, and the two divergent parts of the bare mass. The cross is the insertion $R^2_{\delta,q}$. Since $D^3\ell^{[3]}(0)$ contains the bubble of Figure 11.1, its contraction contains the sunset. Integrating in q turns the crossed line into a line C: the tadpole is linear in N and the sunset logarithmic.

Power counting (Exercise A.3 of Lecture 5) says that no other counterterm is needed. In the flow this is the statement that the integrals (11.8) of all vertices with $k \geqslant 4$ legs converge at $q = \infty$: only the constant mode of the linear jet must be fixed by a boundary condition at a finite scale; its centred part is integrated from infinity like the vertices.

There is a subtlety: the running mass μ_q at fixed q has a limit as $N \to \infty$, but $\mu_N = \mu_\infty$ does not. One never interchanges these two limits. Also, the nonlocal part of the sunset is kept, as the centred kernel $\Theta^{[3]}$ of the corrections: replacing the sunset by its local part would leave a nonlocal remainder of the wrong size.

11.5 Two correction steps

Why two corrections, and not one or three? The answer is in the backward equation of (10.13). Freeze the noise and the large fields, and estimate the size of Z produced by a defect on the ball. The propagator of $\mathrm{d}Z = -HZ\,\mathrm{d}q + \dots$ from q to s is about s/q (since $H \approx C_q$ has norm q^{-1}), so

$$Z_q \approx \int_q^\infty \frac{s}{q}\, b_s\, \mathrm{d}s, \qquad |b_s| \lesssim s^{-1}(\mathsf{S}_4(\mathcal{D}_s)\; r_s^3 + \|\mathcal{E}_s^c\|_{\mathrm{row}} r_s), \tag{11.15}$$

using $\|H_s\| \lesssim s^{-1}$ and that the constant and scalar linear jets of $\mathcal{D}$ vanish, so on the ball $|\mathcal{D}| \leqslant \mathsf{S}_4(\mathcal{D})\|y\|_\infty^3/6 + \|\mathcal{E}^c\|_{\mathrm{row}}\|y\|_\infty$. After n steps $\|\mathcal{E}^c\|_{\mathrm{row}} \lesssim g_s^{n+2}$, so $\|\mathcal{E}^c\|_{\mathrm{row}} r_s \asymp g_s^{n+1}\lambda^{1/2} \asymp \mathsf{S}_4(\mathcal{D}_s) r_s^3$: the linear term contributes exactly like the cubic one, and we follow the latter. After n correction steps the defect is the loop difference of the last two approximations, of relative size g^{n+1}: by the loop estimate,

$$\mathsf{S}_4(\mathcal{D}_s) \lesssim g_s^{n+1} s^{1/2} r_s^{-4} = \lambda^{n+3} s^{-(n+4)/2}, \qquad |b_s| \lesssim \lambda^{n+3/2} s^{-(n+3)/2},$$

and therefore

$$|Z_q| \lesssim \frac{\lambda^{n+3/2}}{q} \int_q^\infty s^{-(n+1)/2} \mathrm{d}s.$$

steps n	$\mathsf{S}_4(\mathcal{D}_s)$	$\lvert b_s\rvert$	$\int_q^\infty \frac{s}{q}\lvert b_s\rvert \mathrm{d}s$
0 (seed only)	$\lambda^3 s^{-2}$	$\lambda^{3/2} s^{-3/2}$	∞ (power)
1	$\lambda^4 s^{-5/2}$	$\lambda^{5/2} s^{-2}$	∞ (logarithm)
2	$\lambda^5 s^{-3}$	$\lambda^{7/2} s^{-5/2}$	$2\lambda^{7/2} q^{-3/2}$

With one step the bounded-field source produces a logarithmically divergent error; two steps are the minimum, and they suffice: $Z_q^{\mathrm{b}} = O(q^{-3/2})$, and the backward energy $\lambda^{-1}\int q^{1/2}|Z^{\mathrm{b}}|^2 \mathrm{d}q$ is finite (Lecture 7). The general (fractional) theory gives the depth criterion

$$(n+2)\,\varkappa > (3+\varkappa)/2,$$

with subcriticality $\varkappa=\frac{1}{2}$ for Φ^4_3: $(2+2)\cdot\frac{1}{2}=2>\frac{7}{4}$, while $n=1$ gives $\frac{3}{2}<\frac{7}{4}$. This is a sufficient condition, which loses $\varkappa/2$; for Φ^4_3 the heuristic above shows that $n>1$ suffices, with $n=1$ borderline.

The two senses of "two renormalisations" are related. The mass counterterm must contain the sunset because the quartic vertex of the corrections, already of the seed, contains the bubble, and contracting it produces the sunset; and the second step is needed because the defect of the first one, the three-loop remainder, is borderline in the backward equation, exactly as the sunset is borderline in the mass.

11.6 The explicit counterterm

Formula (11.11) gives μ_N as an output of the flow, from the boundary value b_*. The input can be made explicit, and this also fixes what the finite part is.

Theorem 11.3. (The explicit counterterm) *Let $a_2=\operatorname{Tr}C_q^2$ and $C_q^{(2)}$ be the kernel of C_q^2; in integrals, powers of kernels are pointwise, $\int C_q^2C_q^{(2)}=\int C_q(0,z)^2C_q^{(2)}(0,z)\mathrm{d}z$. For $|b_*|\leqslant B_0\lambda q_*^{1/2}$ and q_* large,*

$$\beta_q=-\lambda a_2-\lambda\mu_q a_2'+\lambda^2a_2^2+2\lambda^2\int C_q^2C_q^{(2)}+\mathscr{R}_q,\quad |\mathscr{R}_q|\leqslant C\lambda^3q^{-3/2},\tag{11.16}$$

and so, for $f_N(b_*)=\mu_N(b_*)+\lambda\operatorname{Tr}C-\frac{2}{3}\lambda^2\int C^3$,

$$\begin{aligned}f_N(b_*)=&b_*(1+\lambda a_2(q_*))+\lambda(\operatorname{Tr}C-\operatorname{Tr}C_{q_*})\\&-\frac{2}{3}\lambda^2\int(C^3-C_{q_*}^3)+\int_{q_*}^\infty(\mathscr{R}_q+\lambda(\beta_q+\lambda a_2)a_2)\,\mathrm{d}q.\end{aligned}\tag{11.17}$$

Moreover $|f_N(b_{*,1})-f_N(b_{*,2})-(b_{*,1}-b_{*,2})|\leqslant Cg_{q_*}|b_{*,1}-b_{*,2}|$, and $f_N\to f$ pointwise along the whole sequence. Consequently, for B_0 above a universal constant, every $r\in\mathbb{R}$ and q_* large depending on λ,q_0,B_0,r, there is a unique $b_{*,N}$ with

$$\mu_N=r-\lambda\operatorname{Tr}C+\frac{2}{3}\lambda^2\int C^3,\tag{11.18}$$

and $b_{*,N}$ converges along the whole sequence.

Proof. Expansion. Expand $R_0=C-CMC+CMCMR_0$ with $C=C_q$. Since $a_2'=-2\operatorname{Tr}C^3$, the first term of (11.9) is $-\lambda a_2-\lambda\mu a_2'+2\lambda\operatorname{Tr}(C^3\Theta)$, up to $O(\lambda a_2g_q^2)$, and $|\operatorname{Tr}(C^3\Theta)|\leqslant Cq^{-1}v_1(\Theta)$ because $|\hat\Theta(k)|\leqslant 2|k|v_1$. By (11.12) this term is $O(\lambda^3q^{-3/2})$ and goes into $\mathscr{R}_q$. The corrections in $\ell^{[3]}$ give $O(\lambda^3q^{-3/2})$ after contraction, by (11.13). The cubic part of the seed is $-\lambda^2y(x)\int C^2(x,z)y(z)^2$, and contracting its third derivative at zero with R_0^2 gives the operator $\lambda^2a_2\operatorname{diag}(R_0^2)+2\lambda^2C^2\cdot R_0^2$, where $\cdot$ is the pointwise product of kernels. Its constant-mode eigenvalue, with R_0^2 replaced by C^2 at a relative cost g_q, gives the remaining two terms.

Integration. Use $\partial_q\operatorname{Tr}C_q=-a_2$, $\partial_q\int C_q^3=-3\int C_q^2C_q^{(2)}$, and $-\lambda\mu a_2'+\lambda^2a_2^2=-\lambda\partial_q(\mu a_2)+\lambda(\beta+\lambda a_2)a_2$. This is the cancellation of the double-tadpole logarithms: $\beta+\lambda a_2=O(\lambda^2/q)$. At fixed N the boundary terms at $q=\infty$ vanish, which gives (11.17).

Response. For two boundary values with difference δb_*, put $D=\sup_q|\delta\mu_q|$ and $X=\sup_{q,j}q^{3/2}v_1(\delta\Theta_q^{[j]})$, which are finite at fixed N. The loop comparison gives $|\delta\beta_q|\leqslant C\lambda(Dq^{-3/2}+Xq^{-5/2})$ and the centred kernels, outputs of the iteration integrated from infinity, obey $X\leqslant C\lambda^2D$ and $D\leqslant|\delta b_*|+C\lambda q_*^{-1/2}D+C\lambda q_*^{-3/2}X$. Hence $D\leqslant 2|\delta b_*|$, and integrating $\delta\beta$ gives the claim.

Limit and inversion. In (11.17), $\operatorname{Tr} C - \operatorname{Tr} C_{q_*}$ has summable terms $\lesssim (1+|k|)^{-4}$; $C - C_{q_*}$ converges uniformly and $C^2 + C C_{q_*} + C_{q_*}^2$ in L^1; and the integrand converges at fixed q by consistency of the coefficients, dominated by $C\lambda^3 q^{-3/2}$. As $\operatorname{Tr} C - \operatorname{Tr} C_{q_*} \leqslant C + q_*^{1/2}/10$ uniformly in N, the range of f_N contains r for B_0 above a universal constant and q_* large. Monotonicity and pointwise convergence give the convergence of $b_{*,N}$. □

The boundary value b_* is not the finite part: by (11.17), $f_N(b_*) \approx b_* + \lambda q_*^{1/2}/(4\pi)$ at leading order, so at fixed b_*, raising q_* changes the theory.

Exercises

Exercise 11.1. (**Counting loops**) (a) Use (11.5) to show that a loop with p vertices $D^{j_i+1}(U'+\ell)$, $j_i \geqslant 1$, each with $s \leqslant C q r_q^{-j_i}$, and $k = \sum j_i$ external legs has rooted norm $\leqslant C a_2(q) q r_q^{-k} \leqslant C q^{1/2} r_q^{-k}$. (b) Show that $q \cdot q^{1/2} r_q^{-k} = g_q q r_q^{2-k}$. (c) If one vertex is replaced by a vertex of size $\varepsilon q r_q^{-j}$, show that the loop gains the factor ε. Deduce the sizes g^j of the increments $\ell^{[j]} - \ell^{[j-1]}$ in (11.13).

Exercise 11.2. (**The bubble**) Compute $D^3 \ell_q^{[1]}(0)$. Show that its rooted norm is $6\lambda^2 a_2(q)$ and its first spatial moment is $O(\lambda^2 q^{-1})$.

Exercise 11.3. (**Small derivatives are not enough**) On one site take $q = \lambda = 1$, $M = 0$, fixed small $\alpha, \delta > 0$, $\hat\ell_n(y) = \alpha n^{-1}(ny - \sin(ny))$, and $\ell_n = \hat\ell_n + \frac{\delta}{3} y^3$. Show that both have small first derivatives on $|y| < 2$, that $\ell_n - \hat\ell_n$ has bounded derivatives, but $D^3(\mathcal{T}[\ell_n] - \mathcal{T}[\hat\ell_n])(0) = 12(2\delta + \alpha\delta n^2 + \delta^2)$ is unbounded in n. Conclude that the loop estimate needs the individual higher derivative bounds.

Exercise 11.4. (**Why two steps**) Verify the table above. With one step, show that the bounded-field part of Z is of size $q^{-1}\log(T/q)$ on $[q, T]$, for an upper scale cutoff T.

12 The flow at large fields

12.1 The large-field problem

All the estimates of Proposition 11.2 hold on the field ball $\|y\|_\infty < 2 r_q$, and only there. But the forecast Y_q is a random field on N^3 sites, and nothing prevents it from being larger than r_q somewhere. The free field has typical size $q^{1/4} \ll r_q$, but it exceeds r_q with small, nonzero probability, and nothing a priori controls the interacting forecast. We need a force $\bar{\mathcal{F}}_q$ defined and *uniformly coercive for all fields*, which agrees with $\mathcal{F}_q^{\mathrm{o}}$ for $\|y\|_\infty \leqslant r_q$.

A scalar model. The difficulty is already visible in the one-site seed, $\ell_q^{[1]}(y) = \lambda y[(q + \lambda y^2)^{-1} - q^{-1}]$. Its power series in y has radius of convergence exactly r_q: the singularities are at $y = \pm i r_q$. Truncating it at any order produces a polynomial whose leading coefficient alternates in sign: half of the truncations destroy the monotonicity of $U' + \ell^{[1]}$ at $|y| \gg r_q$. The exact function is harmless: it is linear at large fields, and $|\ell_q^{[1]\prime}(y)| \leqslant \frac{9}{8}\lambda/q \leqslant 2\lambda/q$ for all y. In field theory we do not have the exact function, only bounds on the ball, obtained through an expansion of the loop in vertices (the corrections are not polynomials, but their estimates are expansions in the field). This is the large-field problem: perturbative control holds for $|y| \lesssim r_q$, and outside one needs a non-perturbative replacement that preserves the structure the estimates use.

The structure to preserve is coercivity, and it is carried by the bare cube. In the scalar model the coordinate equation $q y + \frac{\lambda}{3} y^3 = q\,\Phi_q$ has noise coefficient

$$H_q(y) = \frac{1}{q + \lambda y^2} \leqslant \frac{1}{q} \wedge \frac{1}{\lambda y^2};$$

large fields are *more* elliptic and less noisy. A good large-field extension keeps U untouched and freezes only the correction.

12.2 Clipping

Let $\tau:\mathbb{R}\to\mathbb{R}$ be smooth and odd, $\tau(u)=u$ on $[-1,1]$, constant outside $[-2,2]$, with $0\leqslant\tau'\leqslant 1$, and set

$$\kappa_q(y)(x):=r_q\tau(y(x)/r_q),\quad \tilde\ell_q(y):=D\kappa_q(y)\ell_q^{[3]}(\kappa_q(y)),\quad \bar{\mathcal{F}}_q(y):=U'(y)+M_qy+\tilde\ell_q(y). \tag{12.1}$$

The clip acts pointwise in space and maps every field into the ball, and the factor $D\kappa_q$ is what keeps the clipped force a gradient. The cubic and linear parts are not clipped. By the chain rule, with factors $|\kappa_q^{(b)}|\leqslant Cr_q^{1-b}$, the clipped correction obeys the same bounds (11.4) globally:

$$s(D^{j-1}\tilde\ell_q)\leqslant Cg_qqr_q^{2-j}\quad(j=2,3,4),\qquad s(D\partial_q\tilde\ell_q)\leqslant Cg_q, \tag{12.2}$$

for all $y\in H_N$; the scale derivative includes the motion of the clip, $\partial_q\kappa_q=O(r_q/q)$.

Lemma 12.1. (Global coercivity) *For q_* large, for all $y\in H_N$ and $q\geqslant q_*$,*

$$\begin{aligned} c\ (K_q+\lambda y^2)\leqslant H_q(y)^{-1}&\leqslant C\ (K_q+\lambda y^2),\\ \|H_q(y)\|_{p\to p}\leqslant\frac{1+C(g_q+g_q^2)}{q}\quad(1\leqslant p\leqslant\infty),&\qquad \operatorname{diag}H_q(y)^2\leqslant Ca_2(q).\end{aligned} \tag{12.3}$$

Idea. $H^{-1}=K_q+\lambda y^2+M_q+D\tilde\ell_q$, and $M_q+D\tilde\ell_q$ is small relative to K_q: $\|D\tilde\ell_q\|\leqslant Cg_qq$, and M_q is small after multiplication by C_q (the centred kernel is controlled by its first moment, Exercise 12.1). Write $H=(I+G(M+D\tilde\ell))^{-1}G$ with $G=(K_q+\lambda y^2)^{-1}$ and use the Neumann series and Lemma 10.1. □

So $\bar{\mathcal{F}}_q$ is a globally coercive force, and Theorem 10.6 applies.

12.3 The complete defect

On the set $\{\|y\|_\infty\leqslant r_q\}$ the clip is the identity and the defect is $\mathcal{D}^{\mathrm{o}}$, of size (11.14). Outside it, the clipped force does not solve the force equation even approximately in relative terms. For $q\geqslant q_*$ split the drift into its bounded-field and large-field parts,

$$b_q^{\mathrm{b}}(y):=-H_q(y)\ D\kappa_q(y)\ \mathcal{D}_q^{\mathrm{o}}(\kappa_qy),\qquad b_q^{\mathrm{l}}:=b_q-b_q^{\mathrm{b}},$$

and let $\chi_q(y)=1_{|y|>r_q}$ (pointwise) and $t_q(y)=y\,\chi_q(y)$, the field restricted to the large-field set.

Proposition 12.2. (Complete source bounds) *For $q\geqslant q_*$, uniformly in $y\in H_N$, N and $p\in[1,\infty]$,*

$$\begin{aligned}&\|b_q^{\mathrm{b}}(y)\|_p\leqslant C\lambda^{7/2}q^{-5/2},\\ &\|b_q^{\mathrm{l}}(y)\|_p\leqslant C\lambda q^{-3/2}(\|t_q\|_p+r_q^{-1}\|y^2\chi_q\|_p),\\ &\|b_q^{\mathrm{l}}(y)\|_2^2\leqslant C\lambda^4q^{-5}\|t_q\|_6^6.\end{aligned} \tag{12.4}$$

Moreover $\|b_q(y)\|_p\leqslant C\lambda q^{-3/2}\|y\|_p$.

The complete proof is Lemma 21.2 of the Supplement. The first bound is (11.15) with $n=2$: on the ball $|\mathcal{D}^{\mathrm{o}}|\leqslant\mathsf{S}_4(\mathcal{D}^{\mathrm{o}})\,(2r)^3/6+\|\mathcal{E}^c\|_{\mathrm{row}}2r$, and $q^{-1}\lambda^5q^{-3}r_q^3=q^{-1}g_q^4r_q=\lambda^{7/2}q^{-5/2}$: the centred linear part of the defect contributes at the same order as its cubic part. The large-field part is as large as the bound $\lambda q^{-3/2}|y|=(g_q/q)|y|$ on the whole drift (no smallness beyond the factor g_q already present in b), but it is *supported on the large-field set* (up to nonlocal tails controlled by operator bounds). The last bound follows from the second since on $\{|y|>r\}$, $|t|+r^{-1}y^2\leqslant 2r^{-2}|t|^3$, and $(\lambda q^{-3/2}r^{-2})^2=\lambda^4q^{-5}$.

Where the large-field error comes from. Compute the defect of the clipped force and compare it with $D\kappa\,\mathcal{D}^{o}(\kappa y)$. With $z=\kappa_q(y)$, $J=D\kappa_q(y)$ (multiplication by $\tau'(y/r)$), $\ell=\ell_q^{[3]}$, $M'=\partial_q M_q$, and the unclipped response $H^{o}=(K+M+\lambda z^2+D\ell(z))^{-1}$, the difference has four groups (seven terms):

i. the mass term $M'y-JM'z$: the linear part is not clipped, but its flow was computed at z;

ii. the motion of the clip, $JD\ell(z)\partial_q\kappa+(D\partial_q\kappa)^{*}\ell(z)$;

iii. $\lambda(y-Jz)\mathrm{diag}H^2$ and $\lambda Jz\,\mathrm{diag}(H^2-(H^{o})^2)$: the cubic vertex sees y, the correction sees z, and the two responses differ by $\lambda(y^2-z^2)$ and by the chain-rule terms of the clipped derivative, all supported on $|y|>r_q$;

iv. the contraction of $D^2\tilde{\ell}-JD^2\ell(z)$ (the chain rule produces terms with κ'', κ''', supported on large fields) and of $D^2\ell$ with $H^2-(H^{o})^2$.

Each group vanishes if $\|y\|_\infty\leqslant r_q$, and each is bounded by g_q times $|t|$ or $r^{-1}y^2\chi$, in L^p, by the same loop estimates (Section 21.3 of the Supplement; Exercise 12.2 for the one-site version). There is no cancellation to exploit: the clipping error is genuinely of the size $(g_q/q)|y|$ of the whole drift on the large-field set. What saves us is that this set is rarely visited, and its occupation is controlled by the coercivity of the actual dynamics. Lecture 7 controls it through the large-field action (13.7).

The coordinate correction. Finally, write the approximate coordinate equation as

$$K_q\Phi_q=K_q(Y_q+\varrho_q(Y_q))+\tfrac{\lambda}{3}Y_q^3,\qquad \varrho_q(y):=C_q(M_qy+\tilde{\ell}_q(y)),\tag{12.5}$$

using $DU(y)=\frac{\lambda}{3}y^3$. The correction is a small contraction, $\|D\varrho_q(y)\|_{p\to p}\leqslant\varepsilon_q:=C(g_q+g_q^2)$, for all y and $1\leqslant p\leqslant\infty$, and $\varrho_q(0)=0$ by oddness. So, up to a small Lipschitz perturbation, *the forecast is the solution of the cubic elliptic equation* $K_q(Y+\varrho)+\frac{\lambda}{3}Y^3=K_q\Phi_q$ *driven by the field at resolution* q. This is the equation whose coercivity Lecture 7 exploits.

12.4 The force below the auxiliary scale

The force above is built for $q\geqslant q_*$, because its expansion needs g_q small. Nothing below q_* requires a construction: we freeze it. For $0<q<q_*$ set

$$\bar{\mathcal{F}}_q(y)=\bar{\mathcal{F}}_{q_*}(y)+(q_*-q)y.\tag{12.6}$$

Then $K_q+D\bar{\mathcal{F}}_q=K_{q_*}+D\bar{\mathcal{F}}_{q_*}$, so the coordinate equation $K_qy+\bar{\mathcal{F}}_q(y)=K_qx$, at $x=\Phi_q$, reads $K_{q_*}y+\bar{\mathcal{F}}_{q_*}(y)=K_qx$. Thus for $q<q_*$,

$$H_q=H_{q_*},\quad y_q(x)=y_{q_*}(C_{q_*}K_qx),\quad C_{q_*}K_q=I-(q_*-q)C_{q_*}.\tag{12.7}$$

The Itô computation of Theorem 10.6 holds for any such family. So the system (10.13) holds on $[q_0,\infty)$, with $Y_{q_0}=0$ for ν_N: the initial value is deterministic, and no large mass is used. The force is continuous in q and piecewise C^1, which is all that Itô's formula needs. The defect for $s<q_*$ is explicit:

$$\mathcal{D}_s(y)=-y+\mathcal{U}(y),\quad \mathcal{U}(y)=\frac{1}{2}C\,\mathrm{tr}_{H_{q_*}(y)^2}D^2\bar{\mathcal{F}}_{q_*}(y).\tag{12.8}$$

Here $\mathcal{U}$ is the loop part of $\mathcal{D}_{q_*}$; it obeys $\|\mathcal{U}(y)\|_p\leqslant Cg_{q_*}\|y\|_p$, which is part of the proof of the global linear bound of Proposition 12.2 (Lemma 21.2 of the Supplement). Uniformly in N, for $s<q_*$,

$$\|\mathcal{D}_s(y)\|_p\leqslant C\|y\|_p,\quad \|b_s(y)\|_p\leqslant C\|y\|_p,\quad \mathrm{diag}H_s^2\leqslant C,\tag{12.9}$$

with $b=-H\mathcal{D}=H(y-\mathcal{U})$. Here we used $\|H\|_{p\to p}\leqslant C/q_*$. These are all the properties of $s<q_*$ we use. Note that $\mathcal{D}$ jumps at q_*; the jump is harmless, and the measure does not depend on q_*. More precisely $\bar{\mathcal{F}},y,\mathcal{D},b,Y,Z$ depend on q_*, while, with μ_N fixed ($b_{*,N}$ then depends on q_*, Theorem 11.3), ν, ψ, Cov and the law of Φ do not.

Exercises

Exercise 12.1. (**Receiving a centred kernel**) Let Θ be a translation-invariant, even kernel with $\Theta 1=0$. With σ_z the translation by z, $(\sigma_z f)(x)=f(x+z)$, and using $C_q\Theta=\frac{1}{2}\int\Theta(z)\,(\sigma_z+\sigma_{-z}-2)\,C_q\,\mathrm{d}z$, show that $\|C_q\Theta\|_{\mathrm{row}}\leqslant C\,q^{-1/2}v_1(\Theta)$ if $\|(\sigma_z+\sigma_{-z}-2)\,C_q\|_{\mathrm{row}}\leqslant Cq^{-1/2}d(0,z)$. Why is the absolute row mass of Θ not the right quantity?

Exercise 12.2. (**The scalar clipping error**) On one site, let $\ell(y)=-\sigma\lambda^2q^{-2}y^3$ (a cubic correction, σ a fixed number) and $\bar{\mathcal{F}}_q=\frac{\lambda}{3}y^3+\kappa_q'(y)\ell(\kappa_q(y))$. (a) Show that $K_q+\bar{\mathcal{F}}_q'\geqslant q/2$ for all y if $\sigma\lambda\leqslant cq^2$. (b) Show that $b_q=b_q^b$ for $|y|\leqslant r_q$. For $|y|>2r_q$ show that κ_q is locally constant, $b_q^b(y)=0$, and $b_q(y)=-\lambda y(q+\lambda y^2)^{-3}$, the drift of the pure cube. (c) Conclude that on the large-field set the error is the whole drift of the loop term: it is of the same form, for $|y|\approx 2r_q$, as the one-site bound $\lambda q^{-3}|y|$ on the whole drift (the analogue of $(g_q/q)|y|$, with $a_2(q)=q^{-2}$ in place of $q^{-1/2}$), but it vanishes on the ball. Compare with (12.4).

Exercise 12.3. (**Large fields are less noisy**) On one site with $\bar{\mathcal{F}}=\frac{\lambda}{3}y^3$, show that the quadratic variation of Y is $\int H_q(Y_q)^2\,\mathrm{d}q$ and that $H_q(y)^2\leqslant(\lambda y^2)^{-2}$. Simulate the Polchinski process for $\nu=\mathrm{e}^{-\lambda\varphi^4/12}\mu^{1/q_0}$ and plot Φ_q, Y_q and ψ_q.

References

[BCG26] I. Bailleul, I. Chevyrev, M. Gubinelli. Stochastic observables and Wilson–Itô diffusions. In preparation.

[BFS83] D. Brydges, J. Fröhlich, A. Sokal. A new proof of the existence and nontriviality of the continuum φ_2^4 and φ_3^4 quantum field theories. *Comm. Math. Phys.* 91 (1983), 141–186.

[BG20] N. Barashkov, M. Gubinelli. A variational method for Φ_3^4. *Duke Math. J.* 169 (2020), 3339–3415.

[FO76] J. Feldman, K. Osterwalder. The Wightman axioms and the mass gap for weakly coupled $(\Phi^4)_3$ quantum field theories. *Ann. Physics* 97 (1976), 80–135.

[GH21] M. Gubinelli, M. Hofmanová. A PDE construction of the Euclidean Φ_3^4 quantum field theory. *Comm. Math. Phys.* 384 (2021), 1–75.

[GJ73] J. Glimm, A. Jaffe. Positivity of the φ_3^4 Hamiltonian. *Fortschr. Phys.* 21 (1973), 327–376.